NASA TECHNICAL MEMORANDUM

NASA TM X-62,368

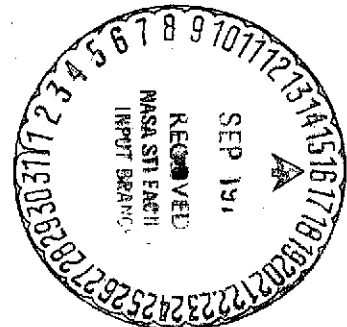## PROPELLER MODULATION EFFECTS ON A SCANNING BEAM

MICROWAVE LANDING SYSTEM

Jack M. Pope and William H. Staehle

Ames Research Center
Moffett Field, California 94035

and

Raytheon Company
Equipment Division
Wayland, Massachusetts 01776

CONTENTS

PROPELLER MODULATION EFFECTS ON A SCANNING BEAM

MICROWAVE LANDING SYSTEM

Jack M. Pope and William H. Staehle

Ames Research Center

SUMMARY

This report presents the results of an investigation to assess the modulation effects on micro-wave signals transmitted through rotating propeller blades. Interruption of the antenna "line-of-sight" signal by the rotating propeller causes a variation of path loss, which produces essentially an amplitude modulation of the received signal. This interruption or blockage effect is generally only partial because of edge diffraction around the particular interfering propeller blade. Signals reflected from the rotating propeller will also cause Doppler frequency shifts to be present in the received signals.

A scanning beam microwave landing system (MLS) known as MODILS (modular instrument landing system) was used to process the received signals for display. The effects of propeller modulation were studied by varying the following parameters:

- Spacing between propeller and receiving antenna
- Propeller dimensions
- Propeller speed (rpm)
- Number of propeller blades
- System data rate
- Receiver response time
- Receiver antenna aperture

A ground station simulator and a variable speed fan with different size blades were used to simulate the actual MODILS ground station and a rotating propeller. Results of the tests are compared with data obtained using the MODILS ground station and the variable speed fan, and also using an actual aircraft whose rotating propeller caused observed propeller modulation.

Data are also presented showing the effects of propeller modulation on a typical Doppler MLS.

INTRODUCTION

Concern about the effects of propeller modulation on microwave signals that pass through rotating propeller blades prompted the Federal Aviation Administration (FAA) to specify a limited series of tests to be conducted by each of the four National Microwave Landing System (MLS) Phase II contractors presently participating in MLS hardware feasibility demonstrations. The extent of propeller modulation investigations undertaken in the Phase II Test Program was, by necessity, very limited because of the myriad of other tests required of each contractor. The MLS Test Requirements and Coordination Plan (ref. 1) documented in section D.8.7.1 specifies locating the static test van antenna approximately 7.6 m behind the rotating propeller of a parked aircraft with the aircraft positioned so that the MLS signals would pass through the rotating propeller blades. Four discrete propeller rpm settings (1500, 1800, 2100, and 2400 rpm) were to be selectively set and the effects on the received signals observed and recorded. Also, the propeller was to be slowly cycled over the speed range to check for any resonance effects due to propeller modulation.

In reviewing this test procedure, it was felt that a more comprehensive test was required in order to clarify the effect of spacing between the receiving antenna and the propeller and to assess the effect of propeller rpm, blade width, data rate, and receiving antenna aperture. These effects are especially important to the general aviation community, particularly the segment concerned with single-engine piston aircraft. Projections are that by 1985 the general aviation fleet size will number approximately 224,000 (ref. 2). Of this number, approximately 78% or 175,000 aircraft will be single-engine piston-powered. In 1973, approximately 40% of the single-engine piston aircraft were four-place (or more) aircraft and 32% of these were equipped with ILS glideslope avionics. Hence, by 1985 potentially about 23,000 single-engine aircraft could be MLS-equipped and some of these could encounter problems due to propeller modulation.

On February 26, 1974, an MLS Interdepartmental Group meeting was held in Washington, D.C. at FAA Headquarters. The purpose of the meeting was to review the initial MLS Feasibility Demonstration data presented by the four Phase II contractors. At this meeting, personnel from the Air Force Flight Dynamics Laboratory of Wright-Patterons Air Force Base presented data concerning the effects of propeller modulation on a Doppler microwave landing system (ref. 3). The effects were so dramatic that it was decided to conduct similar tests on a scanning beam MLS presently installed at Crows Landing, California and being used as the terminal area navigation system in the Joint DOT/NASA STOL Operating Experiments Program. This report describes and analyzes the results of these tests.

SYSTEM DESCRIPTION

A general description of the MODILS scanning beam MLS follows. The basic principle of operation of the ground station and airborne system is described. Specific cycle times and pulse widths are defined and the operation of the ground station simulator is summarized.

MODILS Ground Station

The MODILS system operates through the sequential transmission of microwave beams that scan through the total azimuth and elevation coverage sectors. Angle information is derived in

the airborne receiver through measurement of the time difference between the weighted time centers of a "sync" pulse and the respective received packet of stepped angle beams, as shown in figure 1. The complete angle transmission consists of the transmission of the "sync" signal, the transmission of a vertically oriented fanbeam that steps through the azimuth coverage sector, and then the transmission of a horizontally oriented fanbeam that steps through the vertical coverage sector. The angle information is contained in the fixed relationship between beam-pointing angles and time elapsed since the transmission of the "sync" pulse.

Following transmission of azimuth and elevation angle information, an equal length of time is reserved for distance measurement (DME) operations between the aircraft and ground station. During this time interval, aircraft interrogate the ground station with DME pulses and the ground station replies. Aircraft within the coverage sector measure the time of return of the reply pulses relative to the interrogation pulse to determine the distance from the respective aircraft to the ground station.

In addition to angle and DME transmissions, provision is made for data link transmission from the ground to the aircraft. This transmission takes place during short time intervals that separate the various parts of the angle and DME transmissions. As presently configured, the system transmits a station identification code number during this time interval; however, the transmission of other data can also be accommodated.

MODILS Airborne System

The airborne system consists of the receiver-transmitter (R/T) unit, the control-indicator (C/I) unit, an interface unit, and two antennas, as shown in figure 2. The R/T unit receives and processes the angle information. It also interrogates the ground station and receives and processes the ground station reply to obtain slant-range to station. The control indicator selects station, selects glideslope angle, selects one of three possible azimuth approach angles, and allows adjustment of deviation sensitivity in the event a course deviation indicator (CDI) is used to display angle information to the pilot. The interface unit provides parallel digital angle outputs and a serial digital DME output for processing by a digital avionics system known as the STOLAND system. It also contains circuitry to automatically (or manually) select signals from one of the two airborne antennas, depending upon which antenna is receiving the stronger signal. This feature was added to allow curved, descending STOL approaches to be flown without losing angle or DME navigation information during terminal area maneuvers. One antenna is located in the aircraft nose, and the other antenna is located as far aft as possible, commensurate with minimizing antenna cable losses.

MODILS Ground Station Simulator

The MODILS ground station simulator transmits microwave signals similar to those received at selected points within the ground station coverage sector. Digital timing signals are generated within the unit to control a multifrequency microwave source. Figure 3 is a block diagram of the simulator, and shows the basic operating principle with timing waveforms. A crystal oscillator controls the basic timing of this unit. The outputs of the shift register are trigger signals that control four pulse generators. These generators produce the sync and guard (message) signals, an azimuth signal, and an elevation signal. These signals are routed through a switching matrix under control of the format control and station identification word generator, and they exit on one of four lines (labeled f_1 through f_4 in figure 3) which activate one of the four frequencies of the

microwave source. The signals shown adjacent to the four lines illustrate the timing of the system. The interval between the pulses of line f_1 is 25,800 μs, the basic MODILS repetition interval. The wider pulses on f_2 are azimuth and elevation signals and the narrow pulses are DME replies, while the signals on f_3 and f_4 are station identification transmissions. A simple C-band receiver detects DME interrogations from the airborne system, and is used to trigger a narrow pulse generator, which produces the range replies.

Time differences representing several different azimuth and elevation angles and several slant-ranges to station are selectable to permit operational tests of the airborne system. As the simulator is portable and self-contained, it may be used for flightline preflight tests, maintenance, calibration, and bench repair of the airborne system. Additionally, performance tests on certain portions of the MODILS ground station can be made using the simulator rather than the complete ground station. In fact, use of the simulator for these tests is preferred because of its much lower output power.

Comparison data were later taken at Crows Landing using the actual ground station scanning beam azimuth transmitter instead of the simulator. Results of the comparison are presented and the experimental test setup is discussed below.

DATA

This section presents data obtained using the propeller modulation experimental test setup and also using the MODILS ground station installed at Crows Landing. Data are also presented showing the effects of propeller modulation on a typical Doppler MLS.

Propeller Modulation and Effects on a Scanning Beam MLS

Preliminary analysis — To predict the type of errors and their relative magnitude, a thorough understanding of the system operation of MODILS is required.

The MODILS airborne receiver derives angle information by measuring the time difference between the centers of energy of the frame sync pulse and the respective angle pulse. DME distance is obtained by a similar time difference measurement between the interrogation signal and the DME reply from the ground station. Internal transmitter and receiver delays and the roundtrip signal transit time are accounted for in the receiver signal processing.

These time-multiplexed signals are tracked by four digital servotracking loops. Energy is sampled during two adjacent periods by early and late split gates and then integrated by two integrators. The outputs of the integrators are compared and any difference generates an error signal, which is used to reposition the split gates until each one samples the same amount of energy. The center of energy of each pulse is then tracked and a repositioning of the split gates occurs if the center of energy shifts for any reason.

Essentially, the only difference between each of the four tracking loops is the total gate width between the early and late split gates and the width of the pulses sampled. Table 1 summarizes these differences.

4

TABLE 1.– COMPARISON OF TRACKING LOOPS

Tracking loop	Pulsewidth/beamwidth	Total gate width
Frame sync	300 μs	300 μs
Azimuth angle	246 μs beams	624 μs
Elevation angle	328 μs beams	776 μs
Range	2 μs	2 μs

Figure 4 shows the received azimuth angle video signals, and the azimuth early and late split gates positioned to track the center of energy of the received video signal. The elevation tracking loop is similar, and differs only in the widths of the beams and split gates. Shown at the bottom of this figure is the video signal received from the ground station simulator. Rather than a stepped beam, the simulator generates a single wide pulse of constant amplitude, which is similar to that obtained when the receiving antenna is located midway between adjacent beams in the stepped beam system. The slightly different pulse shape does not materially affect overall airborne system operation since the energy center is the same in either case.

MODILS uses frequency multiplexing to uniquely identify the various signals transmitted. Actual angle and range information is time-encoded by amplitude-modulating the particular frequency involved. The main receiver bandwidth is sufficiently wide to pass all frequency-multiplexed information. Individual receiver sections then allow only certain signals to be passed for further processing.

A rotating propeller causes a slight amount of Doppler frequency shift or frequency modulation (FM) to occur in any reflected signals captured by the receiving antenna. Because of the wide receiver bandwidth (approximately 100 kHz), these frequency shifts have no noticeable effect on receiver output. Only large frequency changes adversely affect system operation.

The major effect of propeller modulation is to cause a variation in path attenuation by periodically blocking or partially blocking the line-of-sight signal path between the transmitting and receiving antennas. Because of edge diffraction around the propeller blade at microwave frequencies, the blockage, in general, is not complete. Also, the blockage effect does not occur instantaneously because of the finite rotational speed of the propeller. Therefore, the pulses become distorted as the blade rotates through the line-of-sight signal path. This distortion causes a momentary shift in the center of energy of the individual received pulses, resulting in a momentary error in the MODILS indicated angle or range. Within the response times of the various tracking loops, the greater the rate of change of attenuation, the greater the individual pulse distortion and the greater the resultant displayed error.

The MODILS airborne R/T unit utilizes digital servotracking loops to track the center of energy of the four individual pulses. The effects of a single error cause an error of one bit. A one-bit error would equal 0.1° in azimuth angle, 0.01° in elevation angle, or 0.005 nmi (9.26 m) in range. Should the error persist, the magnitude of the displayed error increases. This requires the propeller rpm to be equal to (or very near) some multiple of the basic system data rate. The exact value of this "interference" rpm is given by:

5

$$I_f = \frac{60R}{N} \tag{1}$$

where

I_f = fundamental interference rpm

R = data rate (Hz)

N = number of propeller blades

Integral multiples of this interference rpm also cause errors to occur. For example, with a 5-Hz data rate and a three-bladed propeller, the interference occurs at 100 rpm and every 100 rpm encountered above this value. For the unmodified MODILS, the basic data rate is 38.76 Hz; therefore, with a two-bladed propeller, interference occurs approximately every 1162.8 rpm. Unless otherwise stated, the remainder of this preliminary analysis refers to a 38.76-Hz data rate scanning beam MLS system with propeller modulation being caused by a two-bladed propeller operated at a speed of 1162.8 rpm.

Figure 5 is a typical plot of received signal strength versus angular position of the propeller blade. Also shown is the relative pulse amplitude at selected propeller positions. When the propeller is located at either the 180° or 360° points, path loss is near maximum and received signal strength is near minimum because either the first or second propeller blade is directly interposed in the line-of-sight signal path. Note that although the pulse is greatly attenuated, it is either not distorted or it is symmetrically distorted; hence, the center of energy is not shifted. This is also true at the 90° or 270° points, where neither blade interrupts the signal path. At a blade position of 30° or 210°, the slope of signal strength attenuation produces a pulse distortion that causes the center of energy to shift right of pulse centerline; at the 150° or 330° points of propeller rotation, the slope of signal strength attenuation causes the center of energy to shift left of pulse centerline. The net result would be an error that would deviate plus or minus about the nominal receiver output with maximum error occurring where the slope of signal strength attenuation is maximum.

Propeller modulation can also cause errors when the propeller rpm is not exactly synchronized with some multiple of the basic data rate. The exact variation of propeller rpm that can produce an observable error is dependent on the shape of the signal strength curve (with modulation effects present) and the various tracking loop dynamics. For the pulse distortion to be tracked and create an observable error, it must occur within the basic response time of the appropriate tracking gates.

To predict the effect that the propeller modulation shown in figure 5 would have on the pulsewidth and data rate of the MODILS, it is necessary to proceed with the following analysis.

Referring to figure 5, at approximately 150° of rotation, the value of ΔS (which represents change in path loss) is −8 dB and the value of $\Delta\theta$ (which represents the change in angular position of the propeller blade) is about 22°. This represents 12% of the basic modulation period of the MODILS cycle time of 25,800 μs, or 3100 μs. Since ΔT is 3100 μs, the value of $\Delta S/\Delta T$ is then 0.0025 dB/μs.

During this 3100-μs interval, $\Delta S/\Delta T$ remains essentially constant. From the figure it can be seen that $\Delta S/\Delta T$ is also maximized during this interval. It is now possible to predict the error caused by distortion during this time period.

First, consider the DME pulse, which is 2 μs wide. With a $\Delta S/\Delta T$ of 0.0025 dB/μs, the pulse distortion is only 0.005 dB, which would cause the center of energy of the pulse to shift approximately 2.5 ns. This corresponds to a range error of less than 0.9 m. The least significant MODILS range bit represents 0.005 nmi or 9.26 m. Therefore, this amount of distortion causes no observable error. However, the increased attenuation decreases the signal-to-noise ratio and could cause a complete loss in the DME signal.

Next, consider the effect on the Frame Sync (FS) signal, which is 300 μs wide. The slope across the pulse would be 0.775 dB, and this would cause the tracking loop to shift the split gates as shown in figure 6. The actual shift of the center of energy is only 6.63 μs, but the recentered pulse is now reduced in size by the split gates, which have the same width (300 μs) as the FS pulse. Shifting the tracking gate center moves the gate to one side, and 6.63 μs on one side of the pulse is no longer sampled. This results in a new tracking error, causing the tracking loop to move even further left. This process continues asymptotically to a final energy center shift of 11.4 μs. Since angle information is transmitted in the MODILS system as the time difference between the center of energy of the FS signal and the two stepped-beam angle signals, the distortion of the FS signal causes an error in both the azimuth and elevation angles simultaneously. The scale factor of time to angle differs for the two angles: azimuth is 60 μs/$°$, and elevation is 200 μs/$°$. Thus, the effect of the 11.4 μs error in the frame sync tracking would be an 0.19$°$ azimuth error and 0.057$°$ elevation error.

With the actual ground station, it is much more difficult to calculate the effect of propeller modulation on the received azimuth or elevation signal. This is due to the fact that the signal is made up of several beams, and as many as four beams may be within the total width of the tracking gates at any particular angle, as shown in figure 7. Figures 7A and 7B show the received video at two indicated angles within the coverage sectors. The effect of propeller modulation of the given value may cause an azimuth error as small as 0.16$°$ (the case in figure 7A) or as much as 0.30$°$ (the case in figure 7B). The amount of error is thus also dependent upon the arrangement of the beams (or the measured angle). The simulator provides a signal that does not have this variation. Under the same conditions, the receiver would indicate an azimuth error of 0.19$°$. The simulator signal is shown in figure 7C. All three azimuth error values are based on the assumed $\Delta S/\Delta T$ of 0.0025 dB/μs. The corresponding elevation errors would be 0.049$°$, 0.090$°$, and 0.058$°$, respectively. The difference in magnitudes of the azimuth and elevation error is due to the scale factor differences in the two angle functions.

The least significant bit in azimuth is 0.1$°$, while the least significant bit in elevation is 0.01$°$. As the tracking loops are only permitted to move one bit per sample, it is possible to determine the rpm range near the "sync speed" of 1162.8 rpm, where the propeller modulation error is displayed. In the case given in the previous paragraph, the elevation error using the simulator was 0.058$°$, or about six bits. Therefore, to fully display this peak error, the modulation effect must remain for six samples (six pulse recurrence intervals, or $6 \times 25,800 = 154,800$ μs).

As shown in figure 5, $\Delta S/\Delta T$ varies from a minimum to its maximum value of 0.0025 dB/μs in approximately 3 percent of the MODILS cycle time, or 770 μs. $\Delta S/\Delta T$ then maintains this maximum value for an additional 3100 μs. The total time for this variation is 3870 μs. To track the angle error to its peak value on a cycle-by-cycle basis, the allowable interference cycle time variation can be no greater than 25,800 μs $\pm$ 3870/6. This corresponds to an rpm change from 1134 to 1193 rpm, or a difference of 59 rpm. Within this rpm range, the error would be tracked, and in six cycles would be displayed at its maximum value. At rpm values beyond this range, the

7

tracking loop would have insufficient time to track out to the peak error, and thus the displayed error would be less.

The point at which the error would be twice as large as the tracking loop noise can be found by noting the noise level (typically ±2 bits) and doubling this value. This gives the error that the tracking gates must be able to track. Knowing that the loops can move one bit per cycle, it can be seen that the interference cycle time must be 25,800 $\mu s \pm 3870/4$. This corresponds to an rpm range of 1121 to 1208 rpm or a total span of 87 rpm. Within this rpm range, the propeller modulation error is detectable above the tracking loop noise level and can be tracked out to the peak error.

It should be noted that the first rpm range (59 rpm span) varies with the magnitude of the error, while the second range (87 rpm span) does not. Both ranges vary with the duration of the propeller modulation distortion, with a greater percentage of cycle distortion giving the tracking loop longer to track out to a peak error. Additionally, this gives a wider rpm range over which to display the peak error.

In the example above, if the elevation error had been increased to 0.25°, the propeller rpm range needed to display the peak error would be reduced to a range of 1155.8 to 1169.8 rpm, a span of only 14.0 rpm.

It should also be noted that displayed errors may be larger or smaller than predicted, because the Frame Sync signal may be distorted at the same time as an angle signal. The two errors may then add, subtract, or even cancel.

From the preceding discussion, it is apparent that the peak value of error is a function of the rate of change of attenuation ($\Delta S/\Delta T$). The greater the value of $\Delta S/\Delta T$, the greater the value of displayed error. The larger the duration of a discrete value of $\Delta S/\Delta T$, the greater the rpm can vary about the sync speed and still have the peak error indicated. Finally, the greater the change in path loss S, the poorer the signal-to-noise ratio. It should be mentioned that discussions in this paper have not considered errors that may be caused by a decreased signal-to-noise ratio, as this error is normally very minor or nonexistent. At greater ranges, the decreased signal-to-noise ratio can result in noisier angle and DME outputs, but because of the averaging effect of a typical pilot's indicator, little if any error is seen by the pilot.

Calculations were made to determine the effect of multiples (M) of the fundamental interference rpm I_f. To display an error due to propeller modulation, the tracking gates must sample the same distortion segment for a number of consecutive sample cycles. The required number of cycles is dependent upon the peak value of the error. As discussed earlier, a minimum of four cycles is required to reliably indicate any error above the noise level of the tracking loops.

As the effect of increasing the multiple of I_f is to decrease the period of distortion by the ratio $1/M$, and the distortion must remain for the same minimum of four cycles, it may be seen that the allowable step change of the tracking loop is reduced by the ratio $1/M$. Additionally, as there are now M periods of distortion between each system cycle period, this step change is further reduced by the ratio $1/M$. The resultant allowable step change between the propeller period and the system cycle period is reduced by $1/M \cdot 1/M = 1/M^2$. The allowable period T_A to track a minimum detectable error then becomes

8

$$T_A = N \left(\frac{T_S}{M} \pm \frac{\Delta T_f}{M^2} \right) \qquad (2)$$

where

T_A = allowable period to track a minimum error (sec)

T_S = system cycle period (sec)

M = integer multiple of propeller rpm

ΔT_f = allowable tracking loop step change at I_f (sec)

N = number of propeller blades

This formula may be expressed in terms of allowable propeller speed change, ΔP_S, where

$$\Delta P_S = \frac{120}{N} \left[\frac{\Delta T_f}{T_S{}^2 - \left(\frac{\Delta T_f}{M}\right)^2} \right] \qquad (3)$$

If $T_S \gg \Delta T_f$ (as is generally the case), then ΔP_S becomes essentially independent of the value of M (for a fixed number of propeller blades).

Another effect of the multiple M is to increase the peak error. This is due to the fact that the error is caused by the slope of the attenuation $\Delta S/\Delta T$. Increasing M reduces T, and this increases $\Delta S/\Delta T$. The peak error increases to a maximum when the period of distortion is equal to one-half the sample period of the system. This causes the greatest amount of asymmetry to exist in the sampled portion of the received signal. As the sample period differs in each of the four tracking loops, the peak error of each loop differs for different values of M.

To predict the probability of interference occurring with a 5-Hz data rate system (the data rate used by MLS), the MODILS system was changed from 38.76 Hz to 4.845 Hz rate by disabling the angle tracking loops seven cycles out of eight. This resulted in a reduction of the allowable range of propeller speeds by a ratio (in this case) of eight to one, as there were now eight periods of distortion between consecutive samples. Based on the example given previously (which gave an 87-rpm interference band at an I_f speed of 1162.79 rpm for the 38.76 Hz system), changing to a 4.845-Hz system would reduce the interference band to 87/8, or 11 rpm — about the same 1162.79 rpm value of I_f. Changing the data rate to 4.845 Hz also gave a new value for I_f of 145.35 rpm for the same two-bladed propeller, or 96.90 rpm for a three-bladed propeller. But as shown above, increasing the multiple M does not materially affect the allowable propeller speed change, ΔP_S, whereby a minimum detectable error can be displayed. Again using the previous example, it may be seen that approximately 11 rpm out of every 145.35 cause errors to be displayed when using a two-bladed propeller and the MODILS modified to operate at a system data rate of 4.845 Hz. This represents an approximate error probability of 1:13. If a three-bladed propeller were used, approximately 11 rpm out of 96.9 would cause errors and the error probability would increase to 1:9.

If the propeller rpm is an exact multiple of I_f, the displayed error would be constant. If, on the other hand, the propeller rpm were not an exact multiple, the error would vary with time in a cyclic manner.

9

For the MODILS scanning beam MLS, the error period is defined by

$$E_p = \frac{\pm 1}{MR - \dfrac{NP_a}{60}} \tag{4}$$

where

E_p = error period (sec)

N = number of propeller blades

M = integer multiple of I_f

P_a = actual propeller speed (rpm)

R = data rate (Hz)

For example, assume we are within the 87 rpm minimum error tracking band (i.e., $I_f \pm 43.5$ rpm) of the 38.76 Hz standard MODILS data rate and the propeller modulation is being caused by a two-bladed propeller. The value of I_f would be 1162.79 rpm. If the propeller speed were 1200 rpm, the error period would be approximately 0.8 sec. An error of this time duration would probably be ignored by a pilot manually flying an aircraft or by an autopilot because of its built-in filtering. As the propeller speed approaches I_f, the error duration increases and would become more of a problem under either manual or automatic control of the aircraft, particularly during final approach maneuvers.

Now that the basic error producing mechanisms have been described, the independent variables of propeller modulation and the generalized effects they produce will be summarized:

a. Spacing between propeller and receiving antenna affects the slope, duration, and magnitude of attenuation. Total blockage of the signals does not occur because of edge diffraction around the propeller blades. Decreased spacing causes an increase in the slope, duration, and magnitude of signal attenuation with an increase in indicated error.

b. Dimensions of the propeller blades affect the slope, duration, and magnitude of signal attenuation. Increasing the blade width increases the magnitude of $\Delta S/\Delta T$. Increasing the blade diameter reduces the error duration, provided the blade width and distance from the blade tip to the signal interruption point remain constant. Overall results are modified by edge diffraction around the interfering propeller blade and depends somewhat on blade shape.

c. Once well away from the propeller hub (but not near the tip), increasing the radial distance from the propeller hub to the signal interruption point decreases the magnitude of $\Delta S/\Delta T$ and the duration of signal attenuation. This results in a decrease in the magnitude of the indicated error. An increase in edge diffraction effects occurs as the signal interrupt point approaches the propeller tip, causing a further change in indicated error.

d. Multiples of the fundamental interference rpm I_f affect the magnitude of $\Delta S/\Delta T$ and its duration. Increasing the multiple results in a more frequent signal perturbation having less duration. As the duration lessens, $\Delta S/\Delta T$ increases and the error increases up to the point where the tracking gate widths begin to encompass a period of distortion equal to one-half the system sample period.

10

Beyond this point, the error begins to lessen because the degree of signal asymmetry in the tracking gate interval lessens.

     e.   The number of propeller blades affects the lowest interference rpm and its specific multiples as defined by equation (1). Increasing the number of blades lowers the interference rpm because the interference is a function of blade interruptions per minute rather than actual propeller hub rpm. There is an increased probability of error occurring because of the higher number of blade interruptions per revolution of the propeller blade.

The individual system variables (as opposed to those directly relating to the propeller) are now discussed. As before, only the described function is varied; all others are held constant:

     a.   RF frequency affects the slope, duration, and magnitude of signal attenuation. For example, increasing the frequency from C-band (5 GHz) to K_u-band (15 GHz) results in approximately a 3:1 increase in the attenuation effect in accordance with the edge diffraction equations (ref. 4).

     b.   System data rate determines the fundamental interference rpm I_f and the spacing between its multiples. The lower the data rate, the lower the value of I_f, and the more numerous are its multiples. Decreasing the data rate for a fixed value of rpm results in a greater peak error, but a narrower band of rpm values about I_f where interference can occur.

     c.   Tracking rate determines the range of rpm near I_f or its multiples where an error is displayed. The wider the tracking loop bandwidth, the faster its response and the larger the rpm range is to fully display the errors.

     d.   Sample period or tracking gate width determines the absolute error value. When the sample period is short with respect to the duration of maximum $\Delta S/\Delta T$, the shorter the sample period, the less the absolute error. If the sample period is longer than the total duration of the signal attenuation effect, the error is reduced somewhat from its peak value. This case can occur on a low data rate system modulated at a high multiple of the interference rpm. However, this latter case greatly reduces the rpm range around which the peak error may be displayed.

     e.   Characteristics of the receiver AGC exercise control over variations in the received signal strength. The AGC cannot, of course, eliminate propeller modulation completely, but it can keep the signals relatively constant in amplitude at the point in the receiver where detection takes place. This is especially true during the peaks of attenuation, when the signals are attenuated but not badly distorted. Four time-shared AGC loops are used in the MODILS system (one for each tracking loop), but the two angle loops are clamped by the Frame Sync loop AGC. They cannot increase the gain of the receiver much beyond that set by the Frame Sync loop. As angle signals are normally 4 to 6 dB stronger than the Frame Sync signal, this is acceptable. Under certain conditions of propeller modulation, however, (equivalent to ranges in excess of approximately 6 mi) the signal attenuation can exceed this value, and cause a significant reduction in the angle signal-to-noise ratio. Extreme cases may even cause loss of angle lock, as the angle signal becomes attenuated and approaches the noise level of the receiver.

Preliminary data obtained using a single-engine piston aircraft – To assess the effectiveness of the Propeller Modulation Test specified in the FAA Phase II Test Program, a test was conducted at Crows Landing using a Piper Cherokee 6 aircraft, the MODILS ground station, an unmodified

(38.76 Hz data rate) MODILS airborne R/T unit with airborne antenna, and our static test van. The aircraft was parked and positioned so that the received signals were interrupted by the aircraft propeller blades as they rotated. The static test van containing the R/T unit and its antenna was located so that the antenna was approximately 7.26 m behind the rotating propeller, as specified in the Phase II test procedure. Azimuth angle and Frame Sync AGC voltage were recorded on a strip-chart recorder as shown in figure 8. There was an indicated azimuth error of about 0.4° at an rpm setting between 2300 and 2400 rpm; as predicted (e.g., assuming a 38.76-Hz data rate and a two-bladed propeller, the second multiple of I_f is approximately 2325 rpm). There was also a two-fold increase in the peak-to-peak noise level when the propeller was rotating at high rpm compared to when it was stopped.

In figure 8, the plot of AGC voltage, which is a measure of relative signal strength, clearly shows shows the variation of path loss caused by the rotating propeller. This is particularly evident between 2300 to 2400 rpm, and also at idle speed, which is between 1100 to 1200 rpm. The peak-to-peak value of attenuation is approximately 4 dB, which is roughly five times the quiescent AGC noise level.

During the test, it was very difficult to accurately adjust the propeller rpm, and once adjusted it was even more difficult to maintain a particular rpm setting. Although the indicated idle speed of the propeller was about 1150 rpm, it was apparent from the AGC plot in figure 8 that this rpm could not be maintained within ±10 rpm of the desired setting. The actual speed varied from second to second as shown by the period variation of the AGC voltage during idle conditions.

As noted above, this test was conducted using the standard MODILS data rate of 38.76 Hz. To fully assess the effects of propeller modulation, it was felt that a more carefully controlled test was required with the MODILS system data rate degraded to a comparable MLS data rate of approximately 5 Hz.

Propeller modulation experimental test setup — To establish a controlled set of conditions, a laboratory test was devised to study the effect of propeller modulation on the MODILS airborne R/T unit. The experimental setup is shown in figure 9. The ground station simulator was used to transmit the angle and distance-encoded microwave signals through the blades of a variable speed fan that was located at various distances from the receiving antenna. The fan was powered by a variable frequency power amplifier so that a precise adjustment of blade rpm could be made. The receiving antenna was connected to the R/T unit and was located so that the fan blades interrupted the line-of-sight signal path as they rotated. The MODILS airborne R/T unit was modified to update its angle and DME outputs at an approximate 5-Hz rate. The digital angle deviations and Frame Sync signal AGC voltage were recorded on a strip-chart recorder. The receiver intermediate frequency (IF) signals were observed with an oscilloscope and recorded on a video tape recorder. This experimental test setup enabled us to vary the following parameters independently:

- Distance between fan blade and receiving antenna
- Fan blade size
- Fan blade rpm
- System data rate
- Intercept point on the rotating fan blade
- Type of receiving antenna and antenna aperture

12

Effects on the received radio frequency (RF) signals — Figure 10 is a sketch of the receiver RF signals observed at the receiver IF output. Since there is no propeller modulation occurring at this time, there is no pulse distortion and the tracking gates track the exact center of the individual pulses.

Figure 11 shows the effects of severe propeller modulation as would occur in our test setup with the fan blade located 1.22 m from the receiving antenna. This type of distortion occurs as the fan blade slowly strobes through and interrupts the signal path at an rpm near the fundamental interference speed or near one of its multiples. Notice the varying degree of signal attenuation and also the varying slope of $\Delta S/\Delta T$. The effect would be to shift the energy center of the Frame Sync pulse to the left and the energy center of the azimuth pulse to the right, resulting in two errors that would be additive. In the case of elevation signal, the pulse distortion causes a shift in the center of energy in the same direction as the shift in the Frame Sync pulse energy center; therefore, those two errors would be subtractive.

Effects on receiver output data —

Receiving antenna — propeller spacing — The following fixed test conditions shown below in table 2 were established using the experiment test setup.

TABLE 2.— TEST CONDITIONS

MLS transmitter	Ground station simulator
Receiving antenna	6-turn helix with a 7.6-cm reflector
Separation distance between transmitter and receiving antennas	30.5 m
Propeller diameter	76.2 cm
Blade width	10.2 cm
Radial distance to signal interrupt point	33.0 cm
Propeller rpm	Near 1162.8 rpm ($8I_f$)

The spacing between the receiving antenna and the interrupting propeller blades was varied from 0.8 to approximately 8 m in several discrete steps. Receiver AGC voltage and the two angle outputs were recorded on a strip-chart recorder.

Figures 12 and 13 show the effect on receiver outputs when the spacing was at near minimum and maximum, respectively. Peak-to-peak angle and AGC voltage errors are shown. Figure 14 is a combined plot showing the results of this test. Peak-to-peak variations in AGC voltage, elevation angle, and azimuth angle are plotted as functions of the separation distance. Typical angle tracking noise levels (peak-to-peak) are shown for reference. As shown and as predicted in the preliminary analysis, the errors all tend to decrease as the separation distance increases. There was also an unusual nulling effect noted that correlated quite well between these data. Because this null could not be explained by edge diffraction effects or by changing transmitting or receiving antennas, it appeared that perhaps reflections from the surface of our "antenna range" were causing some type of multipath interference effect to also be present. The null was eliminated by adjusting the relative height and position of the receiving and transmitting antennas so that the ground

directly in front of the receiving antenna was not strongly illuminated by the transmitted microwave signals.

A plot of these data is shown in figure 15. The test conditions were the same as before except an antenna with wider aperture was used to provide better capture of any multipath reflections that might be causing constructive or destructive multipath interference. To obtain better null resolution, many more points were taken about the previous null point located at approximately 3 to 4 m spacing.

The figure clearly shows the absence of any nulls. The peak-to-peak error still decreases as the separation distance increases, although the error magnitude is less. This can be explained by the fact that the multipath interference previously noted had been eliminated.

A test was conducted at Crows Landing to determine the effects of propeller modulation on receiver processing of the actual ground station scanning beam signals when the spacing between the propeller and receiving antenna was varied from 0.76 to 6.1 m. The fixed test conditions are shown in table 3.

TABLE 3.– TEST CONDITIONS AT CROWS LANDING

MLS transmitter	Ground station azimuth transmitter at Crows Landing
Receiving antenna	6-turn helix with a 7.6-cm reflector
Spacing between transmitting and receiving antennas	225 m
Propeller diameter	76.2 cm
Blade width	10.2 cm
Radial distance to signal interrupt point	33.0 cm
Receiving antenna height from ground	1.8 m

Referring to figure 16 we see that the plot of peak-to-peak AGC and azimuth angle error still decreases with increasing separation distance. And again we see the effect of multipath ground reflections causing an apparent null at a separation distance of 3 to 4 m. Changing receiving antenna aperture by changing antennas did not change the magnitude of the error or the position of the null.

Propeller dimensions –

a. Propeller width variation: This test was also conducted at Crows Landing with the same fixed conditions shown in table 3 except the separation distance between the propeller and the helix receiving antenna was held constant at 1.22 m and the blade edge distance from the interrupt point was held constant in the radial and tangential directions for each blade by varying the radial distance from the rotational center to the interrupt point. The effect changing the blade width from 10.2 cm to 15.2 cm had on the indicated peak-to-peak path loss and angle variations is shown in figures 17 and 18. The increase in blade width caused the peak-to-peak path loss S to increase from −4 dB to −5 dB. $\Delta S / \Delta T$ also increased, resulting in an increase in peak-to-peak error from 5 to 6 bits. The normal noise

level was 3 bits peak-to-peak; therefore, the increase in indicated azimuth angle error was from ±0.1° for the narrow blade to ±0.15° for the wide blade. The AGC voltage plots display a slight amount of pulse noise and 60 Hz pickup from the portable generator used to supply system power.

b. Radial distance to signal interrupt point: The fixed test conditions were the same as the ones shown in table 2 except the wide aperture, "coffee can" receiving antenna was used, the separation distance between the propeller and receiving antenna was held constant at 2.44 m, and the radial distance from the propeller center of rotation to the signal interrupt point was varied.

The results of this experiment did not closely follow the preliminary predictions. Radial distances of 23.0, 24.0, 35.5, and 38.0 cm were tried. Taking a closer look at the edge diffraction mechanism, it was noted that the diffraction effect of a blade begins even before the edge interrupts the line of sight between the antennas. Radio propagation theory (ref. 4) suggests that there is an effect at least out to the point where the line of sight is three wavelengths or approximately one Fresnel zone away from each blade edge. As the wavelength of the MODILS is 5.761 cm, this effectively occurs as far as 17.3 cm on each side of the blade.

Because of the radial length limitations of the fan blades used in this experiment, we were unable to use a large enough blade where this diffraction region was small as compared to the circumference of the blade arc. Also, the observed effects of edge diffraction were already complicated by the presence of two edges only a few wavelengths apart that were both causing edge diffraction. Hence, the net effect on AGC voltage and angle error was not as severe as originally expected.

Some of the effects may be seen in figures 19, 20, and 21, where the line of sight was located 0 cm, 2.5 cm, and 8.9 cm from the tip of the blade. Although the effect is slight, the peak-to-peak AGC voltage variations and angle errors increased slightly as the interrupt distance from the blade tip increases (or the radial distance from the hub decreases). The upper trace in each figure is AGC voltage and the lower trace is azimuth angle. The peak-to-peak AGC voltage variation increases from approximately 5 to 6 dB as the distance varied from 2.5 to 8.9 cm spacing. Edge diffraction at the tip caused the AGC voltage to increase slightly when the interrupt point was located at the blade tip ($d = 0$ cm). Angle errors increased in number rather than in actual magnitude.

Propeller rpm, data rate, and number of propeller blades — The fixed test conditions were the same as those listed in table 3 except the propeller-receiving antenna spacing was maintained at 76 cm. The propeller rpm was varied from approximately 1160 to 1165 rpm.

Figure 22 is a plot of the data obtained as the propeller rpm was varied over a narrow range about an interference speed of 1162.79 rpm $(8I_f)$. From the period of interference it is possible by means of equation (4) to determine two possible propeller speeds causing the interference. In region A on the figure, the inference period is 14.8 sec. Therefore, the actual propeller speed (from eq. 4) is:

$$P_a = \frac{60(MRE_p \pm 1)}{NE_p} \tag{5}$$

15

$$P_a = 60 \frac{[8(4.845)(14.8) + 1]}{2(14.8)}$$

Therefore, $P_a = 1160.77$ rpm or 1164.83 rpm ($8I_f \pm 2.03$ rpm). In region B, the interference period is 41.2 sec; therefore, P_a must be either 1162.06 rpm or 1163.52 rpm ($8I_f \pm 0.73$ rpm).

These experimental test results show that the interference period is inversely proportional to the difference between the actual propeller rpm and the system interference rpm; as this difference lessens, the interference period becomes larger.

The propeller modulation effect is also shown in figure 8 at two specific rpm multiples. In this instance we were observing the effects of propeller modulation caused by the propeller of a Piper Cherokee 6 aircraft while using the unmodified MODILS whose data rate is 38.76 Hz. With a two-bladed propeller, the first two predicted rpm values where propeller modulation should have been observed were at approximately 1163 rpm and 2326 rpm. The effect is most noticeable on the AGC voltage plot. At approximately 2325 rpm and at idle speed (approximately 1150 rpm) there is a distinct signal strength variation causing an AGC voltage fluctuation whose period is approximately 4 to 5 sec in duration, as indicated by the 1-sec time marks and by the AGC voltage plot shown. This implies that the propeller rpm values were within ± 5 to 10 rpm of the predicted interference values.

Because of the limitations of the laboratory experimental test setup (i.e., inability of the fan motor to rotate long blades at high rpm), further tests to determine the effect of rpm multiples were not conducted.

The only change in data rates was in changing the MODILS from a 38.76-Hz system to a 4.845-Hz system. Most of the laboratory measurements were made either using the ground station simulator or the azimuth scanning beam ground station at Crows Landing with the MODILS configured for the lower data rate (i.e., approximately 5 Hz). Obtaining noticeable propeller modulation at many multiples of I_f was very difficult because of limitations in our ability to accurately maintain low rpm settings with our experimental test setup. As noted before, the interference rpm band becomes much narrower as the data rate is decreased and even more careful control of the propeller rpm is required if peak errors are to be fully displayed.

Actual experimental tests using propellers having more than two blades were not conducted because of excessive loading of the fan motor. For this test, even longer fan blades were required in order to avoid edge diffraction interference between adjacent blades. Also, increasing the number of blades without increasing their length produced an increase in loading to the extent that accurate control of the blade rpm could not be maintained.

Antenna aperture — Very limited experiments were performed to determine the effects of aperture. Initial tests, which consisted of substituting three types of antennas, were complicated by the presence of multipath reflection. As each of the antennas had different beamwidths (i.e., 30° to 300°), various amounts of reflection were encountered. A later test was made with a ground plane reflector placed below and in front of the receiving antenna. A number of measurements were made with the ground plane located from 0 to 30 cm below the slotted waveguide antenna. The reflector was 43 cm wide and 54 cm long and was located so that the rear edge of the reflector was even with the rear edge of the receiving antenna or about 2 cm behind the antenna radiating

16

surface. The effect of the ground plane on the direction characteristics of the antenna was to vary its radiation resistance and also the number of lobes contained in the antenna radiation or receiving pattern (ref. 5). Both of these variables affect the antenna gain and, hence, the effective antenna aperture.

In figure 23, the results of this test show a 3-dB change in the peak-to-peak attenuation value with the maximum attenuation occurring when the ground plane was almost touching the bottom of the receiving antenna. A nulling effect was observed when the ground plane was approximately 10 cm or 1.7λ below the antenna. This implies that propeller modulation effects are minimal at this particular spacing.

The angle errors correlated fairly well with the attenuation curve, although the error changes were quite small and were near the quiescent noise level of the respective tracking loops. Further tests under more controlled conditions are necessary to quantify the effects of antenna aperture on propeller modulation.

Receiver response time – The unmodified MODILS system utilizes a rate-aided tracking loop to follow rapid changes in angle readings as would be encountered when flying at right angles to the final approach course at short distances to the (originally collocated) MODILS transmitter site. Without rate aiding, the loop is a simple two-state, first-order servoloop. If four consecutive samples resulted in error corrections of the same polarity, an up/down counter would generate a rate-aiding signal to compensate for the trend. This would multiply the response of the servoloop up to five times the unaided rate. This higher response rate results in a noiser tracking of the signals. The alteration of data rate (by eliminating certain numbers of samples) also disables the rate-aiding section of the tracking loops, resulting in a simple first-order servoloop. The effect of this can be seen by comparing the tracking loop noise levels with and without rate aiding in figures 8 and 13.

In figure 8, with rate aiding, the azimuth tracking loop noise level is roughly 6 bits or 0.6° peak. In figure 13, without rate aiding, the azimuth tracking loop noise level is about 3 bits or 0.3° peak. As shown, the use of rate aiding essentially has doubled the quiescent tracking loop noise level. During the remaining laboratory experiments with the MODILS modified for a 5-Hz data rate, the tracking loops were kept in the non-rate-aided condition to give a higher "signal-to-noise" ratio. This allowed us to observe smaller error magnitudes caused only by propeller modulation.

The characteristics of the AGC loops were not altered during the tests, as it was not practical to do so. Ideally, these should be independent AGC voltages derived for each sampling interval. In this manner, what happens at one sample (during the Frame Sync period) would not affect actions at another sample (during the respective angle periods). As the system would normally have a gain reserve at any point within a specified range, an independent AGC system would prevent degradation of the signal-to-noise ratio at the receiver output when severe propeller modulation conditions occur. The MODILS AGC loops are not completely independent. As mentioned previously, the angle AGC voltages are dependent on the Frame Sync AGC voltage level. Therefore, the MODILS AGC system has not been completely optimized for conditions of severe propeller modulation.

17

Propeller Modulation Effects on a Doppler MLS

On 30 January 1974, as part of their research with advance landing guidance systems, the Air Force Flight Dynamics Laboratory (AFFDL) at Wright-Patterson Air Force Base conducted a test to investigate the effects of propeller modulation on the quality of the Doppler MLS guidance (ref. 3). A horn antenna was mounted 1.22 m behind the right propeller of a C-131 aircraft and connected by means of a coaxial cable to a Doppler MLS receiver installed in the aircraft.

The normal airborne instrumentation was used to record the MLS data and other parameters as the aircraft was moved to different positions on the taxiway. At each position, the aircraft was aligned so that, as the aircraft propeller rotated, it interrupted the MLS line-of-sight signal path. Data were recorded over a range of engine speeds called out by the pilot from the standard rpm indicator. Figures 24 and 25 are reproductions of these data obtained by AFFDL during the test.

Figure 24 shows an approximate 1° offset bias develops after engine start. The peak-to-peak noise level also increased from 0.1° to about 1°. Figure 25 shows the effect of varying engine speed. There is an azimuth count change equivalent to about 0.6° in azimuth angle as the indicated engine speed was varied from 1000 to 2000 rpm.

It should be noted than the actual blade interruption speed was not the indicated rpm shown by the pilot's indication. Because of gearing, the C-131 propeller hub speed is 0.45 × indicated rpm. Also, the propeller used is typically a three-bladed propeller; therefore, to obtain the actual blade interrupt speed, each of the indicated engine speeds must be multiplied by the factor 3 × 0.45 or 1.35.

According to the AFFDL report cited in reference 3, the azimuth angle errors caused by propeller modulation are thought to be caused by loss of Doppler zero crossings during the angle transmission periods. Other Doppler systems might or might not be affected as severely by this problem.

The important fact that should be noted is that although the antenna was positioned very close to a large propeller (estimated as 30 cm wide at an intercept point 1 m from the hub), the two errors were sustained and they were quite appreciable. Errors of this magnitude could cause considerable problems when operating aircraft at or near ILS minima.

CONCLUDING REMARKS

As a result of the analyses and actual experimental tests conducted, it became apparent that the prescribed propeller modulation tests called for by the FAA are not comprehensive enough to adequately assess the effects of propeller modulation on all the Phase II MLS configurations. Propeller rpm and propeller-receiving antenna spacing are thought to be key parameters in determining how the different MLS receivers respond to the effects of propeller modulation, although propeller dimensions are also important. These two parameters should be investigated more extensively, particularly since the pilot's rpm indicator does not, in general, indicate the actual blade interruptions per minute. Also, the 7.6-m spacing called for is much greater than that which would be typical for single-engine general aviation aircraft, where the major problems caused by propeller modulation will exist.

In comparing the MODILS scanning beam MLS and the AFFDL Doppler MLS performance under severe propeller modulation conditions, it was noted that the probability of a sustained error occurring was considerably higher for the Doppler system. Not only were large bias errors present but there were also errors related to propeller rpm. For large errors to be sustained by the MODILS, the propeller rpm must be at an exact multiple of the system data rate. For large MODILS errors to occur even intermittently, the propeller rpm must fall within a very narrow rpm band about some multiple of the system data rate. The scanning beam system investigated appears to have a much higher tolerance to propeller modulation than the one Doppler system for which data are available, although the 1.2-m spacing used in the Doppler test and the width of the C-131 propeller are rather atypical situations. Also, it is apparent that the observed error magnitude and duration are very system-dependent. For example, a different Doppler MLS configuraiton might have greater tolerance to propeller modulation than the AFFDL Doppler system. Different receiver signal processing techniques could also result in improved system performance.

It might be possible to avoid the problem completely by locating the antenna at a different position on the aircraft so that propeller blockage does not occur. Other possible locations are at the wing tip, on the leading edge of the wing, or at the top of the vertical stabilizer. A study should be conducted to assess the feasibility, cost, and performance tradeoffs involved in locating the antenna at these and other locations. An antenna installation for several general aviation aircraft that considers cable routing, cable losses, and installation cost should be included in the study. Type of antenna and antenna polarization should also be investigated because of their importance in determining overall MLS performance.

There is also the possibility of using a wide aperture antenna located within the propeller shadowing region. As long as the antenna was at least 1.8 m behind the propeller, wider aperture could result in a decrease in the propeller blockage effect and hence fewer propeller modulation errors. Lower cable losses would also be possible with this antenna location.

Location of the airborne antenna at other than the aircraft centerline results in guidance errors. To assess the impact of these errors, it is necessary to review the appropriate Federal Air Regulation (FAR) error limits for a conventional Instrument Landing System (ILS).

FAR171-47 establishes the accuracy requirements of a conventional ILS as those contained in International Civil Aviation Organization (ICAO) Annex 10, Volume 1, Chapter 3. Above the threshold of the runway, the ILS centerline should be within ±10.5 m of the true runway center-line. Attachment C of Annex 10 specifies the accuracy of the airborne receiver as being dependent on the stall speed of the aircraft. For Category I operations, stall speeds of 95 knots or less require receiver centering error no greater than ±13 μA with a 68% probability. This current error may be converted to a distance error of approximately ±28 m. Assuming a proportional increase in error with increasing distance from runway threshold and that the distance errors are additive, the maximum permitted error at a decision height of 60 m (Category I minima) is 54 m. As the distance to touchdown is roughly 300 m, adding 3 to 5 m of offset error by placing the antenna on a wingtip should not materially affect the amount of final course correction required.

Because of additional equipment and personnel requirements (from Advisory Circular 91-16 and FAR Part 61), Category II operations are highly unlikely for light or heavy single-engine aircraft. Therefore, accuracy considerations beyond Category I are not pertinent for these classes of aircraft.

For large aircraft operating with Category II and III capability requiring wide-angle antenna coverage, shadowing of a single antenna caused by the aircraft's body surfaces or appendages may cause a momentary loss in the MLS signals at the airborne receiver and a resultant loss in MLS guidance. This condition may be unacceptable to the pilot and will require multiple antenna locations on the aircraft to eliminate signal dropouts. For such cases, in addition to antenna placement problems, the rationale as to when and on what basis to switch antenna needs further study.

In conclusion, there are several areas for investigation that need further study, some of which might have a major impact on the National MLS Program and could further the usefulness of MLS.

REFERENCES

1. Anon.: MLS Phase II Test Program Test Requirement and Coordination Phase. Dept. of Trans.—Fed. Avia. Admin., September 7, 1973.

2. Anon.: Analysis of the General Avionics Requirements for the 1980's. Interim Presentation to NASA—Ames Research Center, Decision Sciences Corporation, February 14, 1973.

3. Brindley, A. E., Calhoun, Patton, T. H., and Valcik, L.: Analysis, Test, and Evaluation Support to the USAF Advance Landing System Program. Air Force Flight Dynamics Laboratory (AFFDL) TR-74-62. May 1974.

4. Bullington, K.: Radio Propagation Fundamentals. Bell System Technical Journal, vol. 36, no. 3, May 1957, pp. 607-608.

5. Terman, F. E.: Radio Engineers Handbook. McGraw-Hill Book Co., Inc., 1943, pp. 788-790.

"SYNC"-SIGNAL   DIRECTIONAL SIGNALS

t=0

t=1   t=2   t=3   t=m
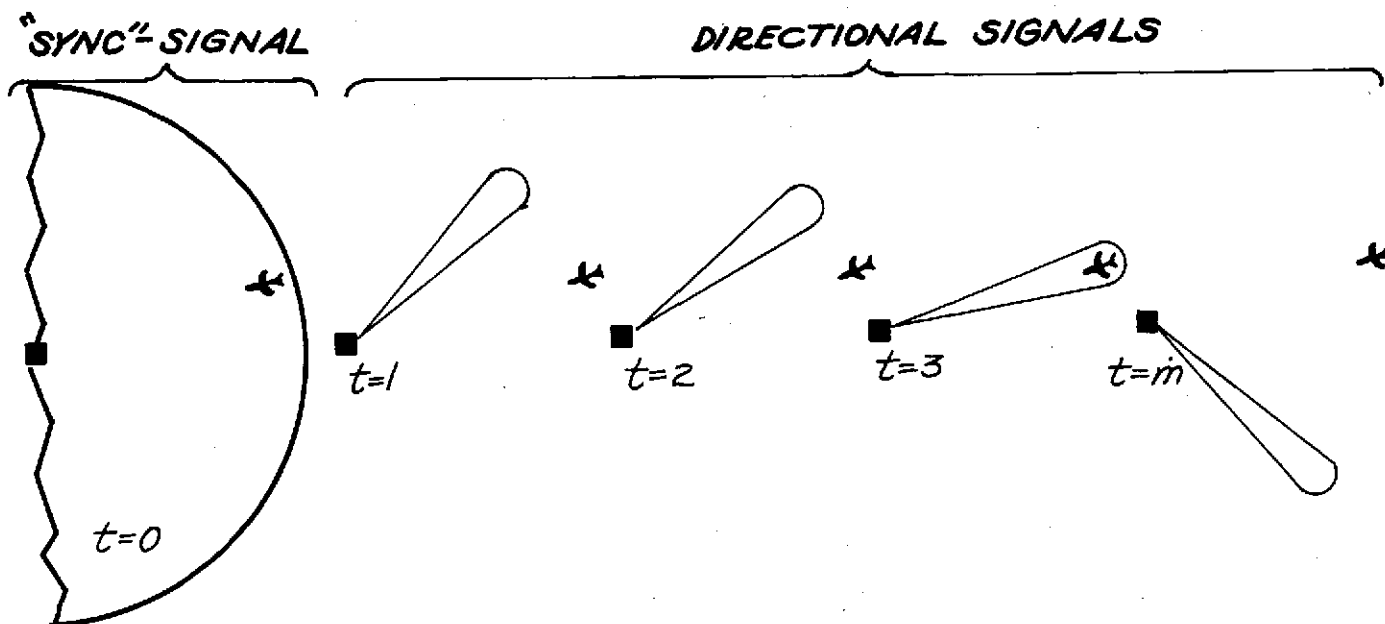
I-A. GENERATION OF LOCALIZER COURSE

WEIGHTED   EQUIVALENT
TIME CENTER   CONTINUOUS BEAM

STEPPED BEAM

AMPLITUDE

t=0   t=3   TIME
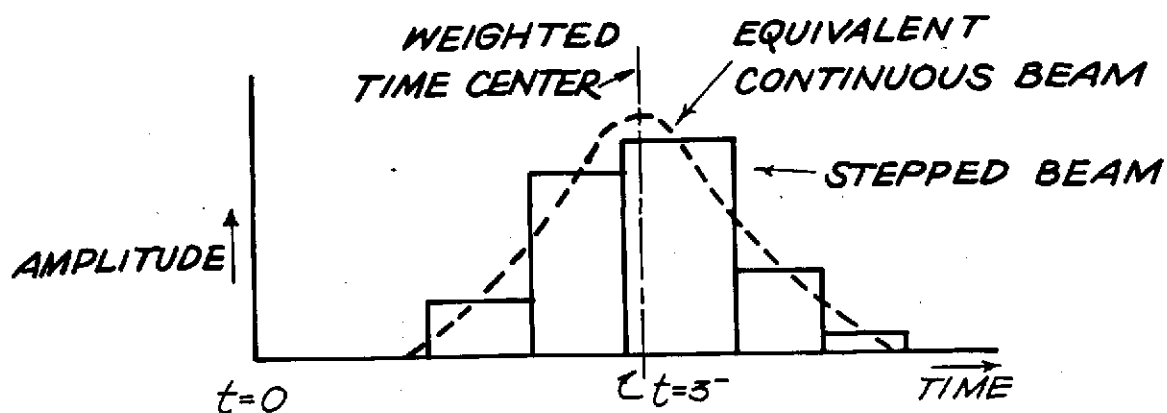
*I-B STEPPED BEAM AND EQUIVALENT
CONTINUOUS BEAM*

*FIGURE I. OPERATION OF MODILS SCANNING
BEAM MLS*
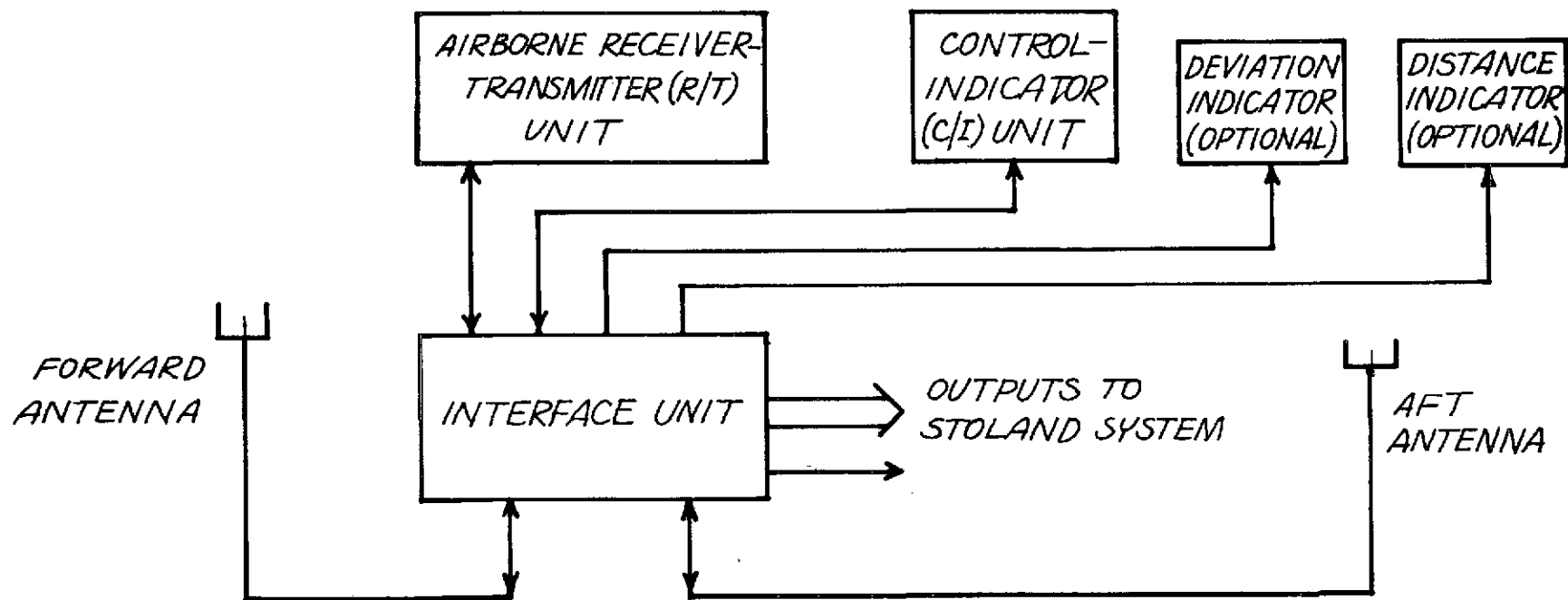
FIGURE 2. MODILS AIRBORNE BLOCK DIAGRAM
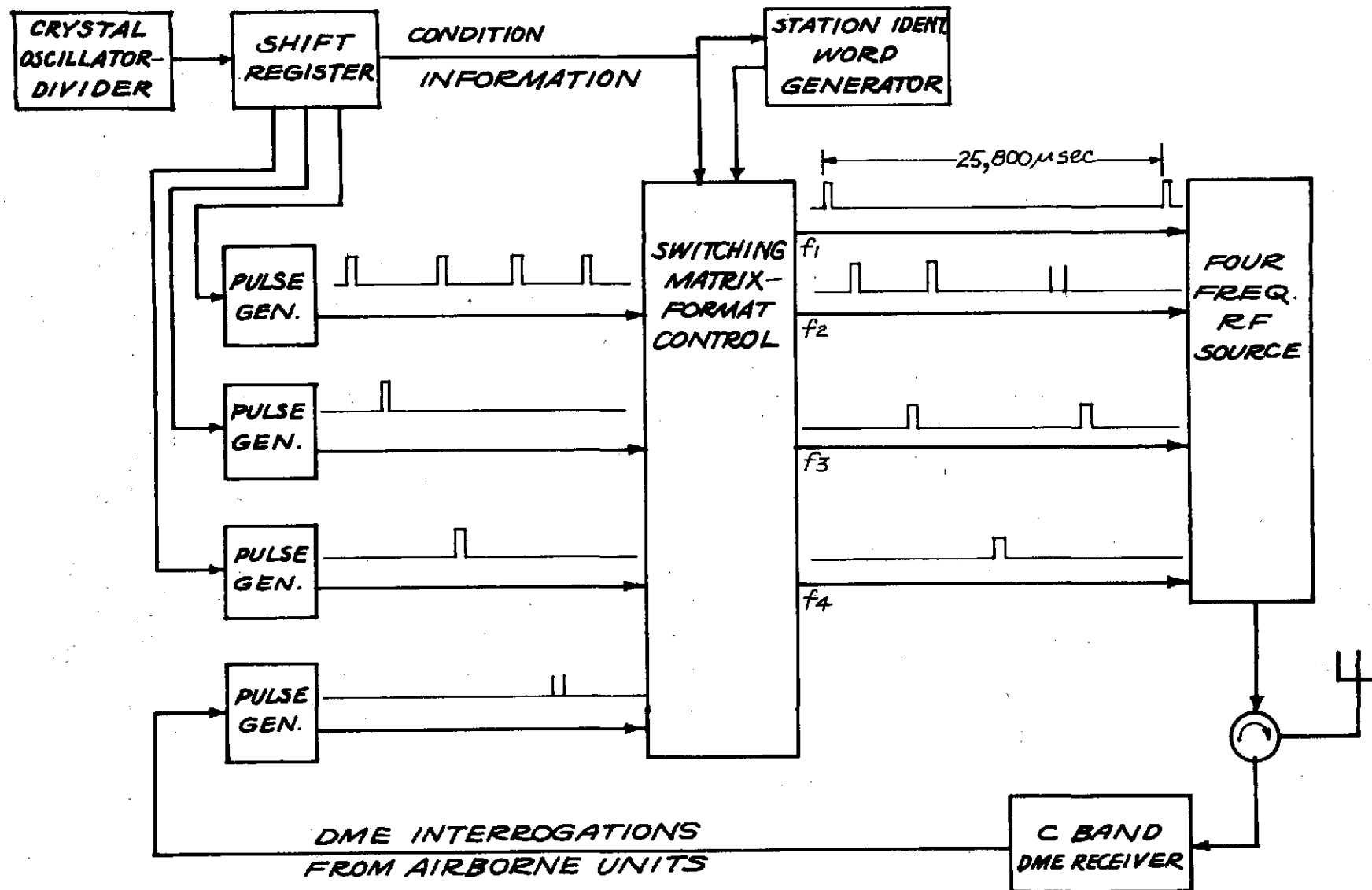
FIGURE 3. MODILS SIMULATOR BLOCK DIAGRAM

CENTER OF ENERGY

246 μsec.   246 μsec.   246 μsec.

RECEIVED AZIMUTH
VIDEO SIGNALS

AZIMUTH EARLY
SPLIT GATE

312 μsec.

AZIMUTH LATE
SPLIT GATE

312 μsec

624 μsec

SIMULATOR
SIGNAL (VIDEO)

530 μsec

SAMPLING
INTERVAL
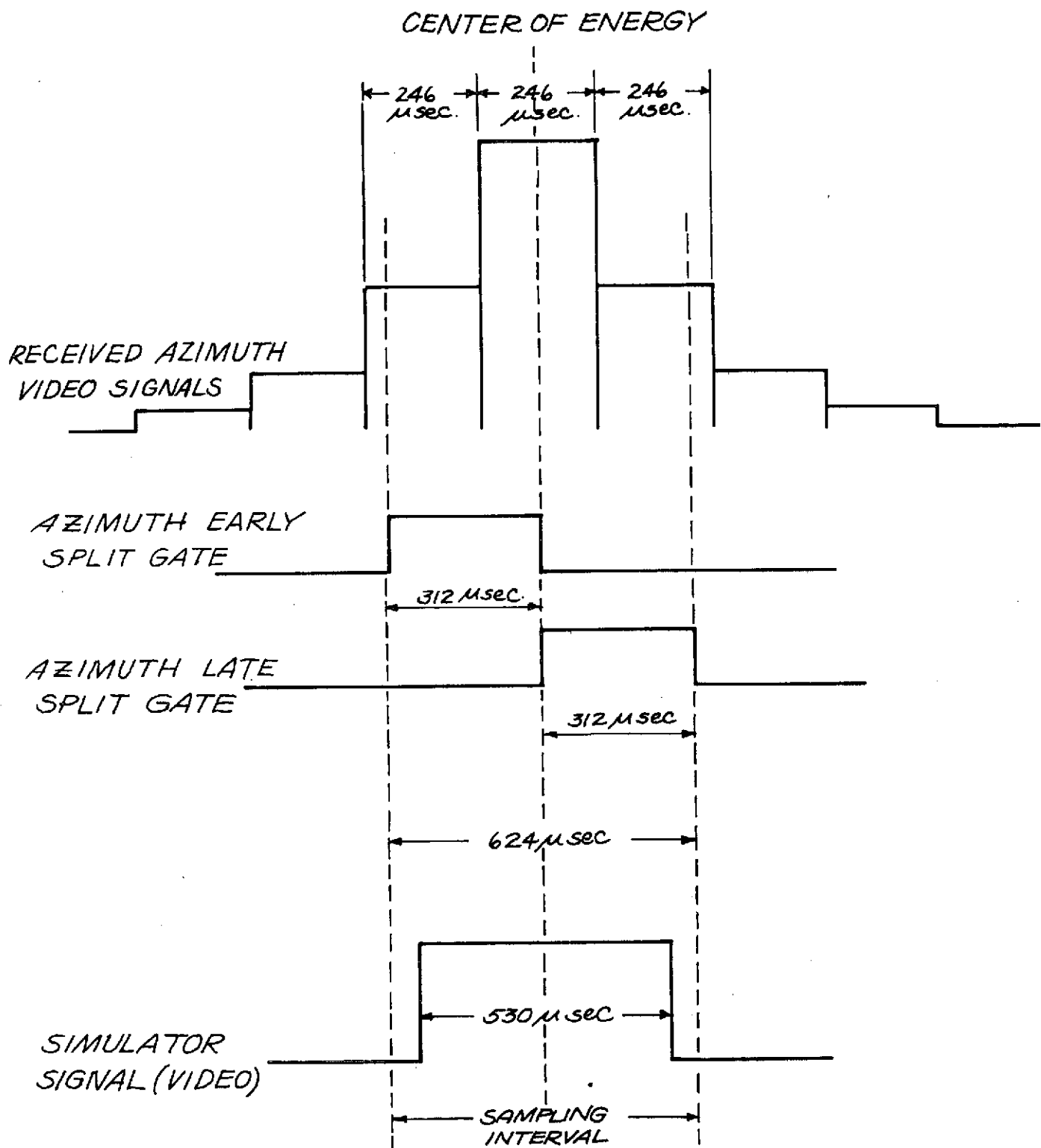
FIGURE 4. AZIMUTH TRACKING GATE SIGNALS
COMPARED WITH RECEIVED AZIMUTH
SIGNALS.
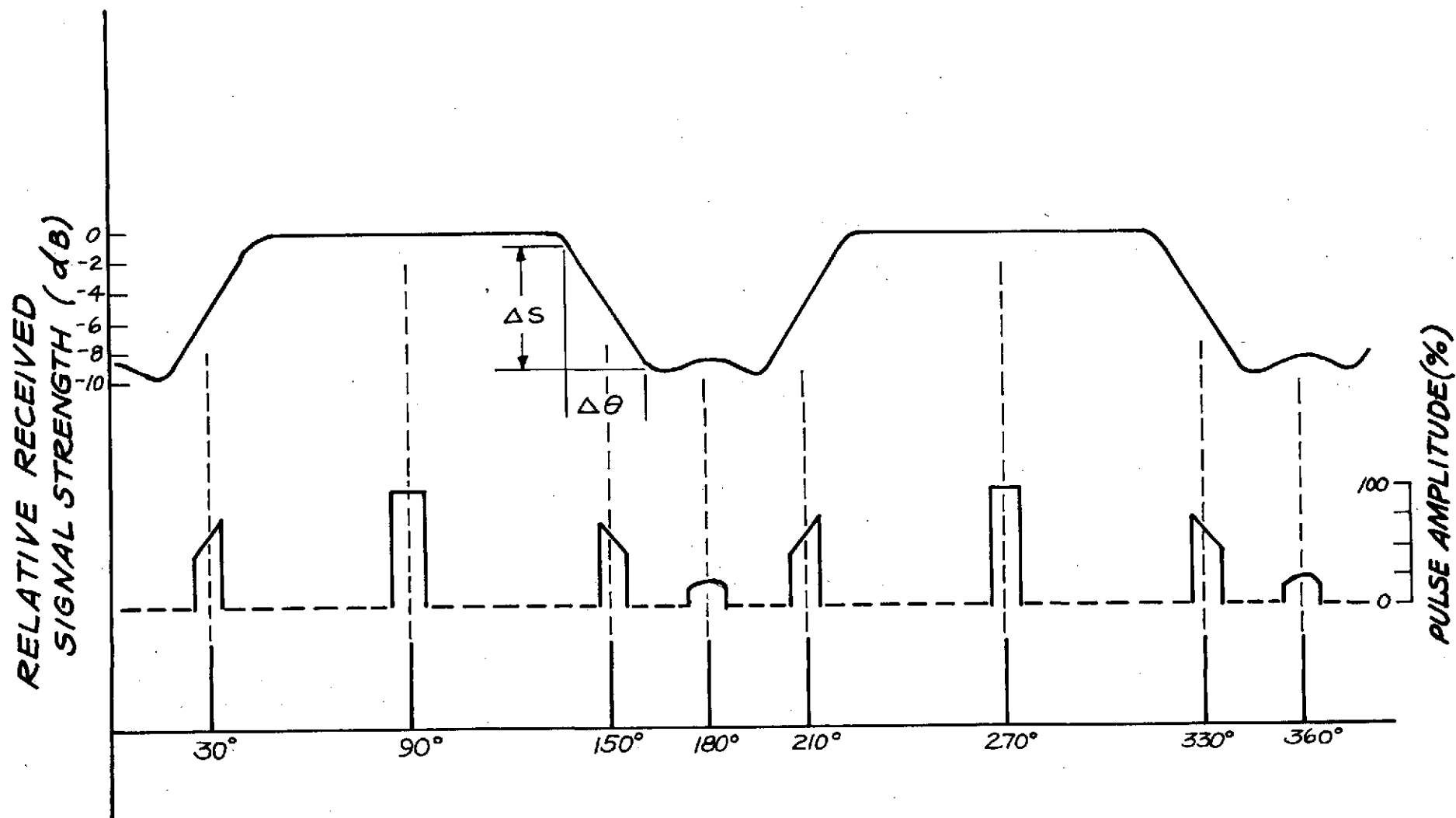
FIGURE 5. RELATIVE RECEIVED SIGNAL STRENGTH, PROPELLER POSITION, AND PULSE AMPLITUDE.

CENTER OF ENERGY OF DISTORTED PULSE

TRUE CENTER OF UNDISTORTED PULSE

$6.631 \mu sec$

$\dfrac{\Delta S}{\Delta T} = 0.0025 \dfrac{dB}{\mu S}$

300 μsec

TOTAL ERROR

11.4 μsec

EARLY SPLIT GATE 150 μsec

LATE SPLIT GATE 150 μsec

6.631 μsec

CENTER OF TRACKING GATES

PORTION OF PULSE NOT SAMPLED
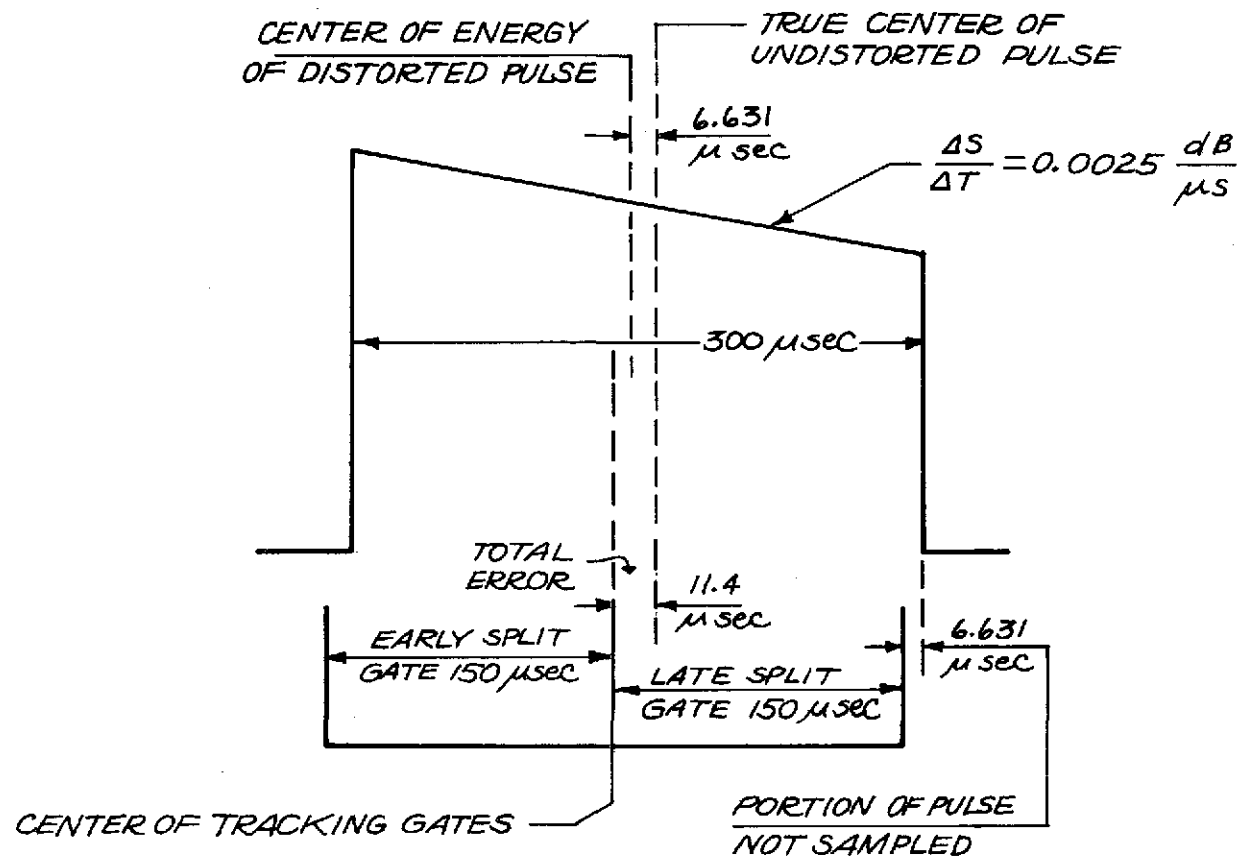
FIGURE 6. TRACKING ERROR CAUSED BY FRAME SYNC PULSE DISTORTION.

CENTER
OF
ENERGY

ANGLE VIDEO

7A

ANGLE VIDEO

7B

SIMULATOR
ANGLE VIDEO

7C

TRACKING
GATE WIDTH
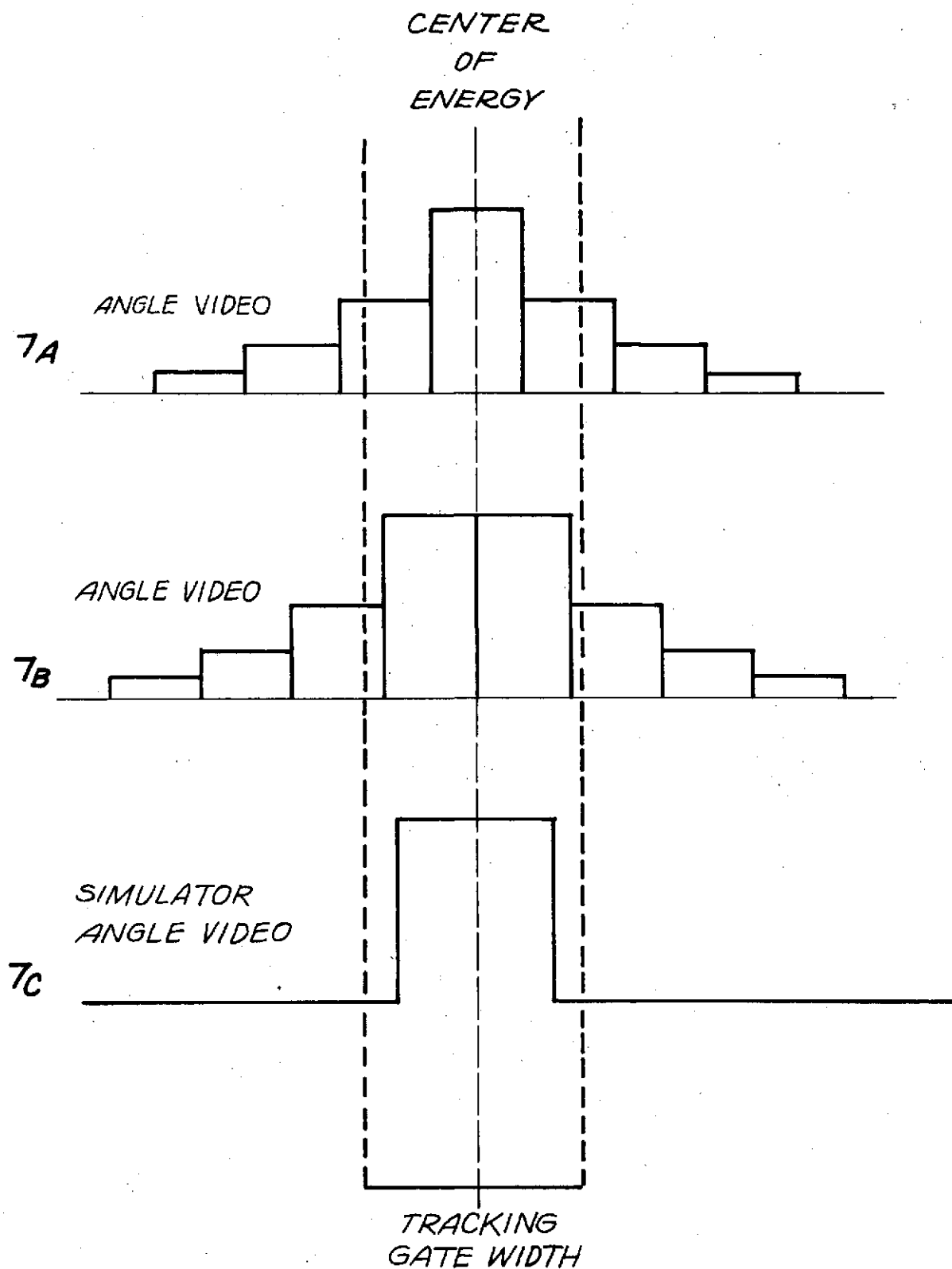
FIGURE 7. - TYPICAL BEAM PATTERNS
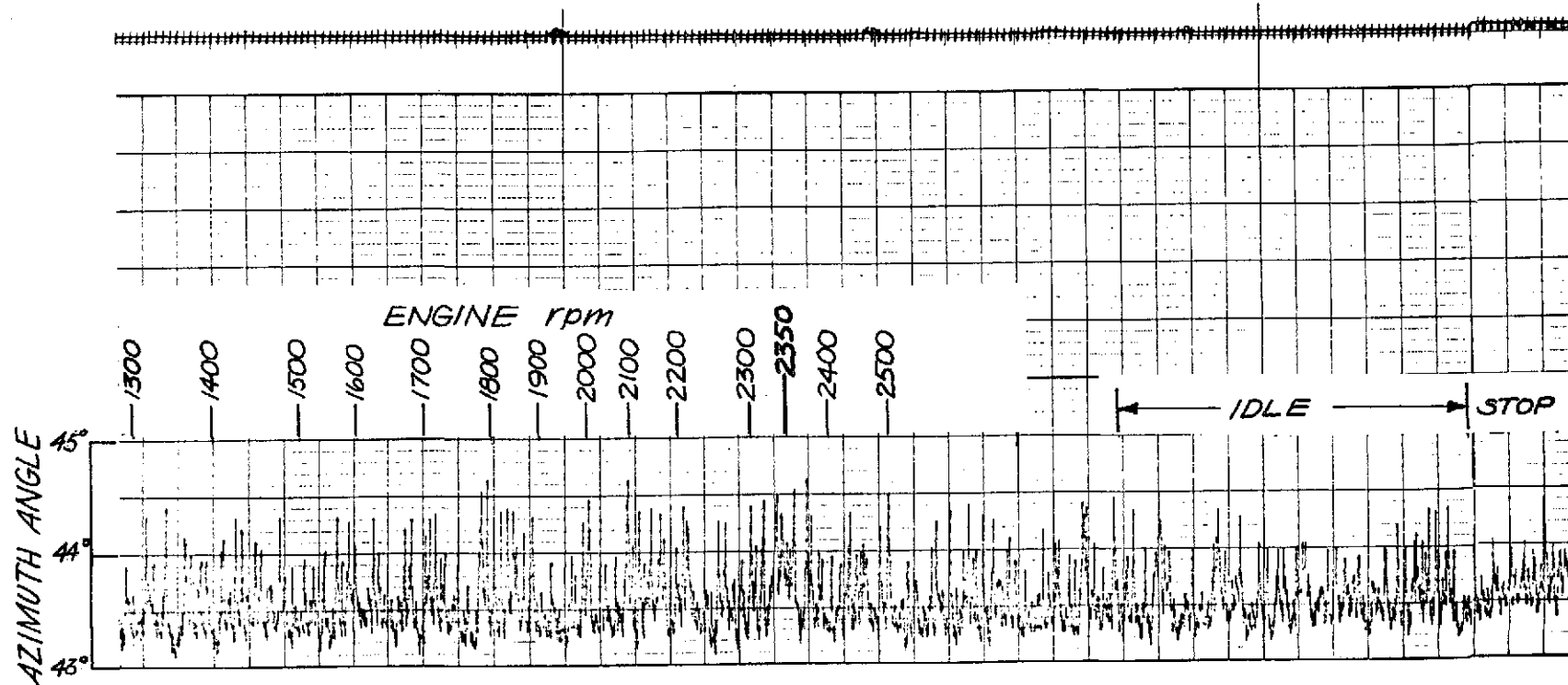
FIGURE 8.-PRELIMINARY PROPELLER MODULATION TEST AT
CROWS LANDING USING A SINGLE ENGINE PISTON
AIRCRAFT AND THE UNMODIFIED MODILS.
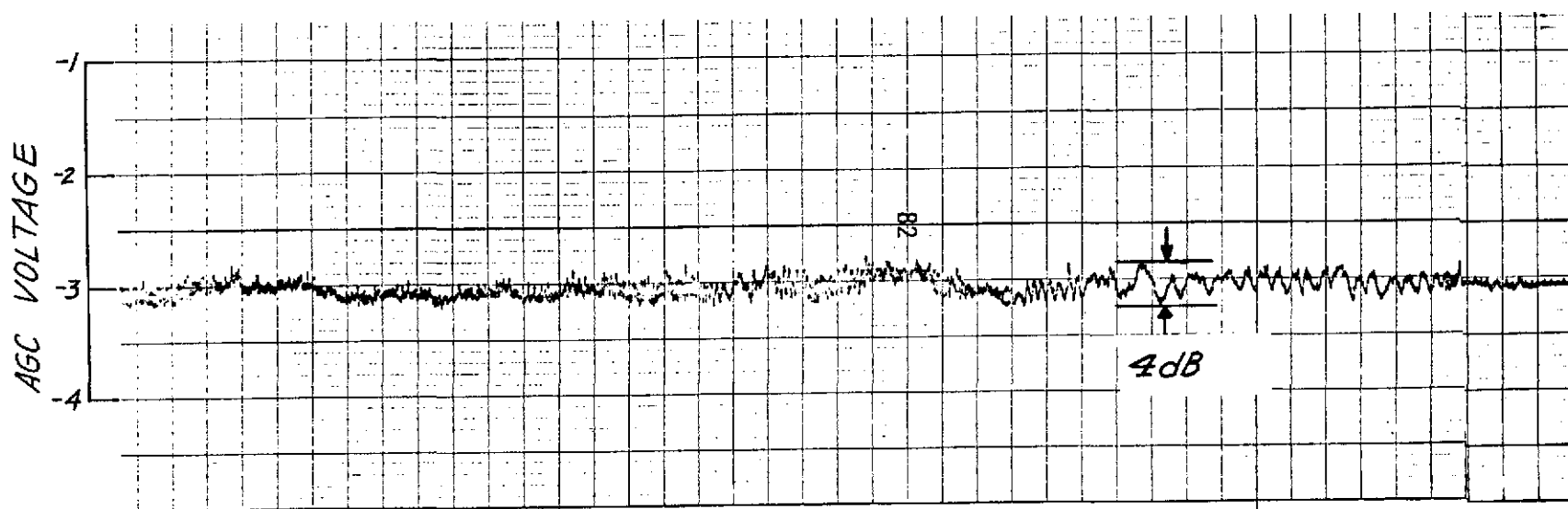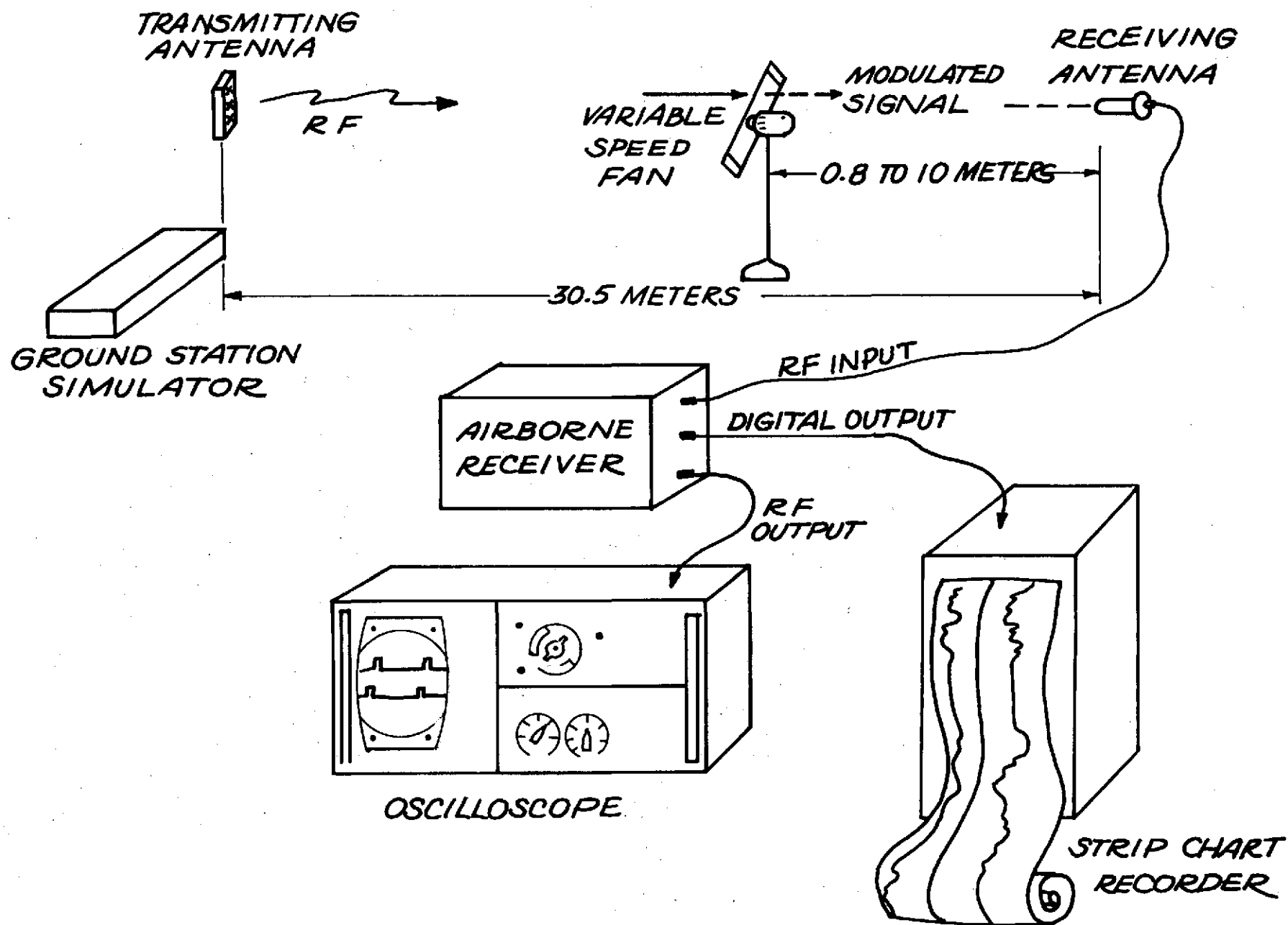
FIGURE 9. PROPELLER MODULATION EXPERIMENTAL SETUP

FRAME SYNC AZIMUTH MESSAGE (STATION IDENT.) ELEVATION

0.4 VOLT

300 μsec
527 μsec
300 μsec
527 μsec

2736 μsec
(2)

7636 μsec
(5°)
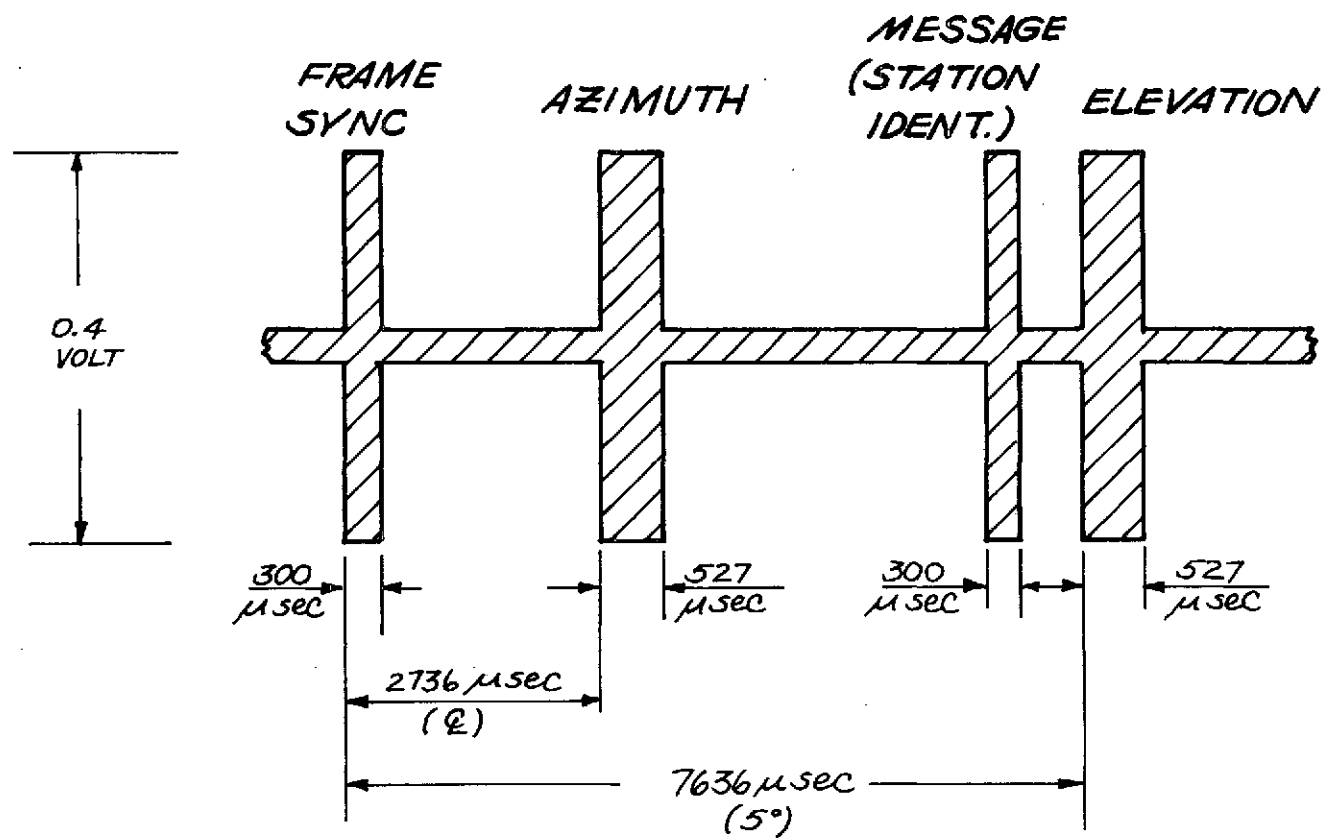
FIGURE 10. RECEIVER "RF" SIGNALS, WITHOUT PROPELLER MODULATION
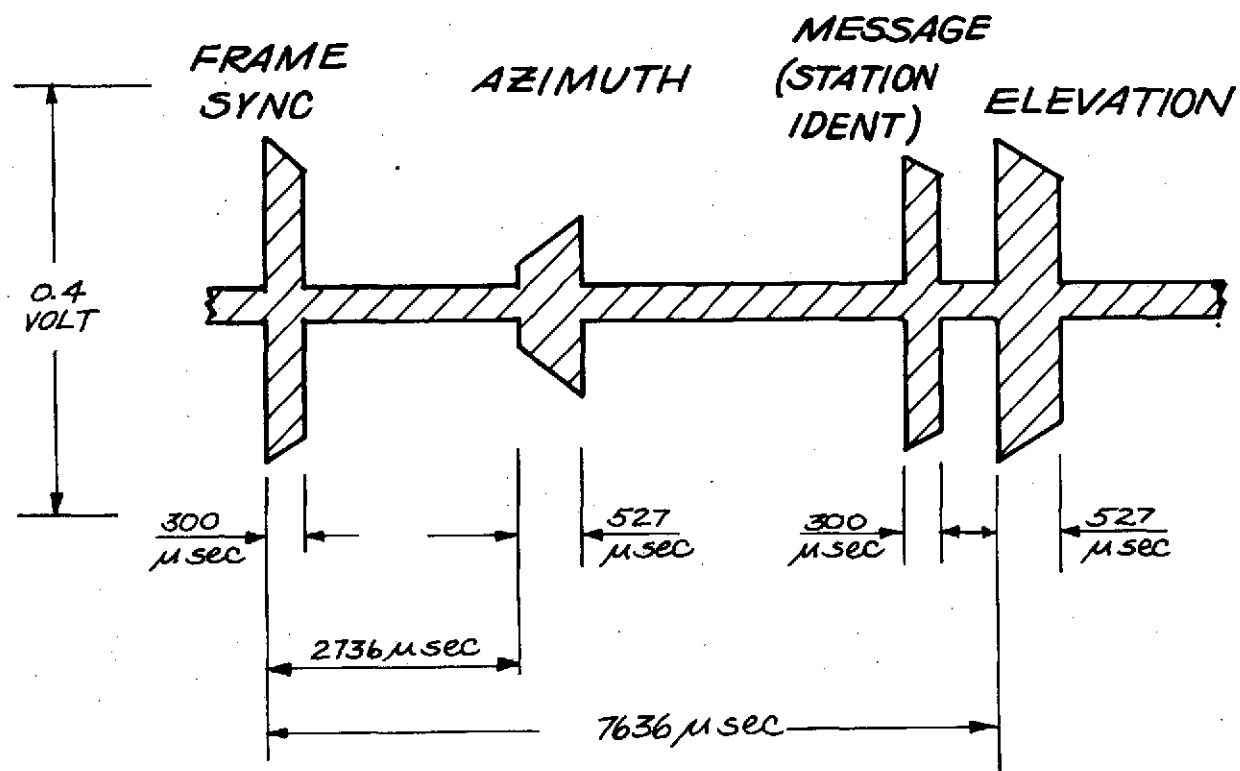
FIGURE 11. RECEIVER "RF" SIGNALS, WITH PROPELLER MODULATION

AGC ERROR   12 dB

AZIMUTH ANGLE ERROR   1.1°

ELEVATION ANGLE ERROR

0.15°
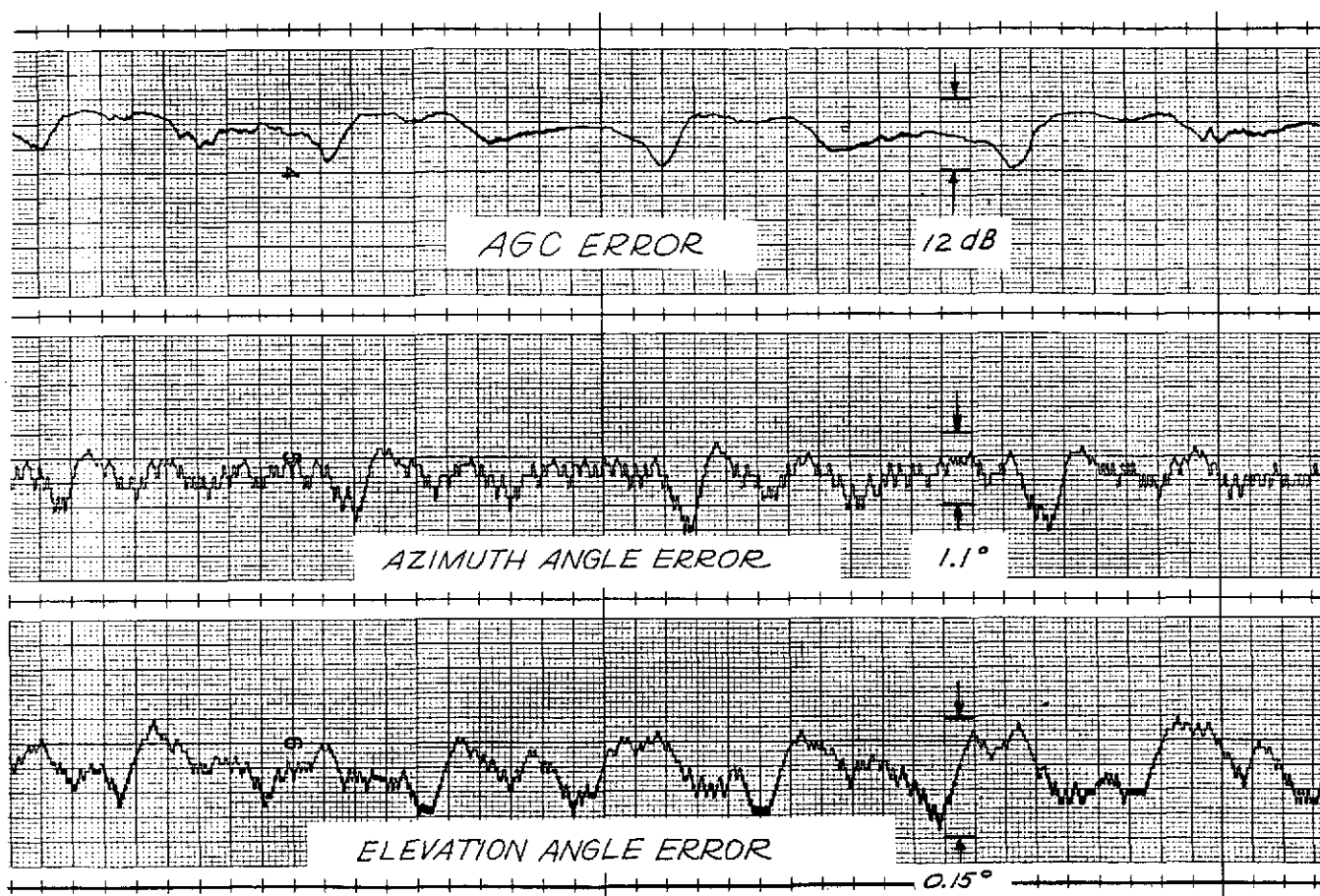
FIGURE 12 - ANGLE AND AGC ERRORS AT
1.4 m SPACING

AGC ERROR   6dB

0.4°

AZIMUTH ANGLE ERROR

0.06°

ELEVATION ANGLE ERROR
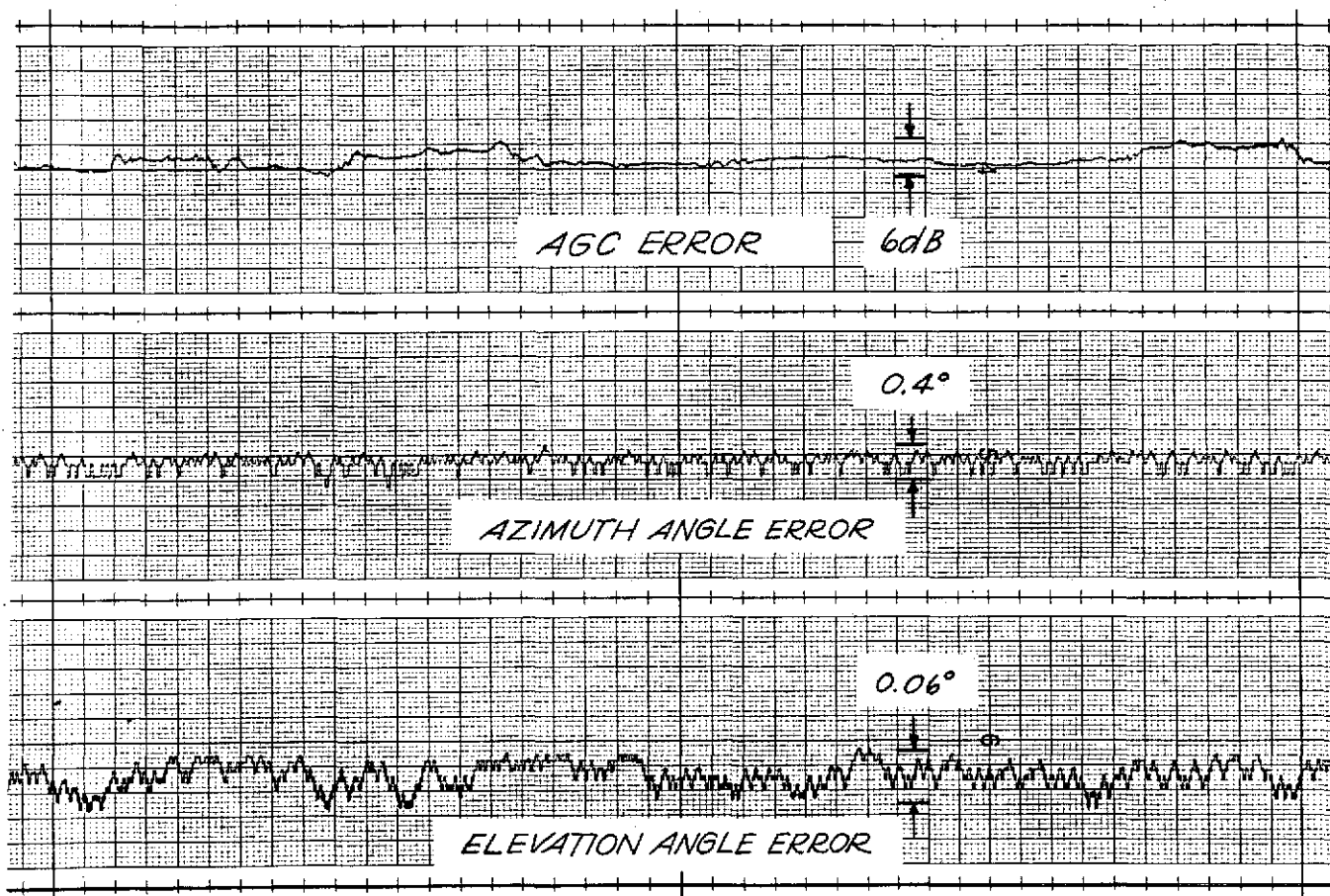
FIGURE 13-ANGLE AND AGC ERRORS AT
8.2 nu SPACING
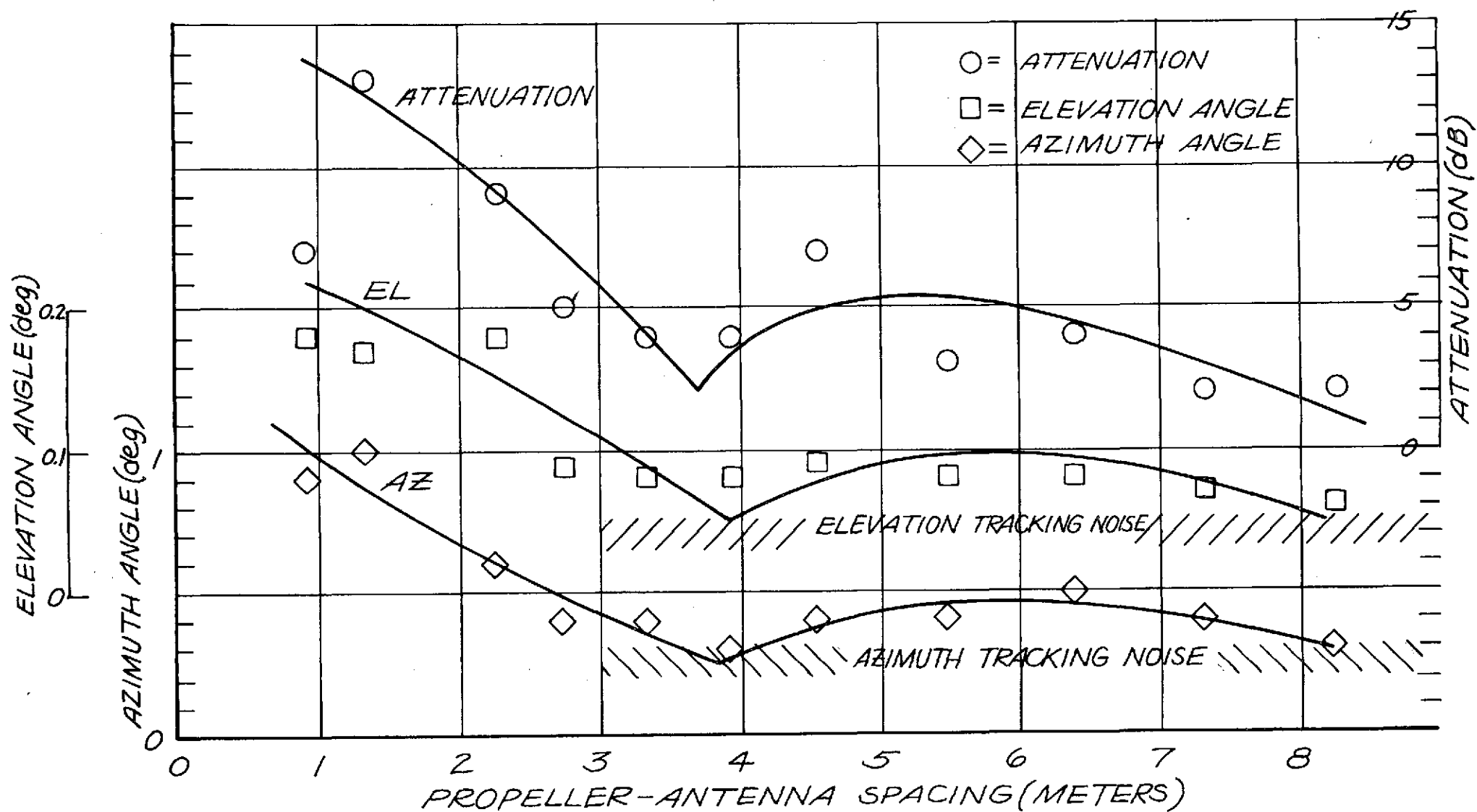
FIGURE 14. AGC AND ANGLE PEAK-TO-PEAK ERRORS
VERSUS PROPELLER-RECEIVING ANTENNA SPACING
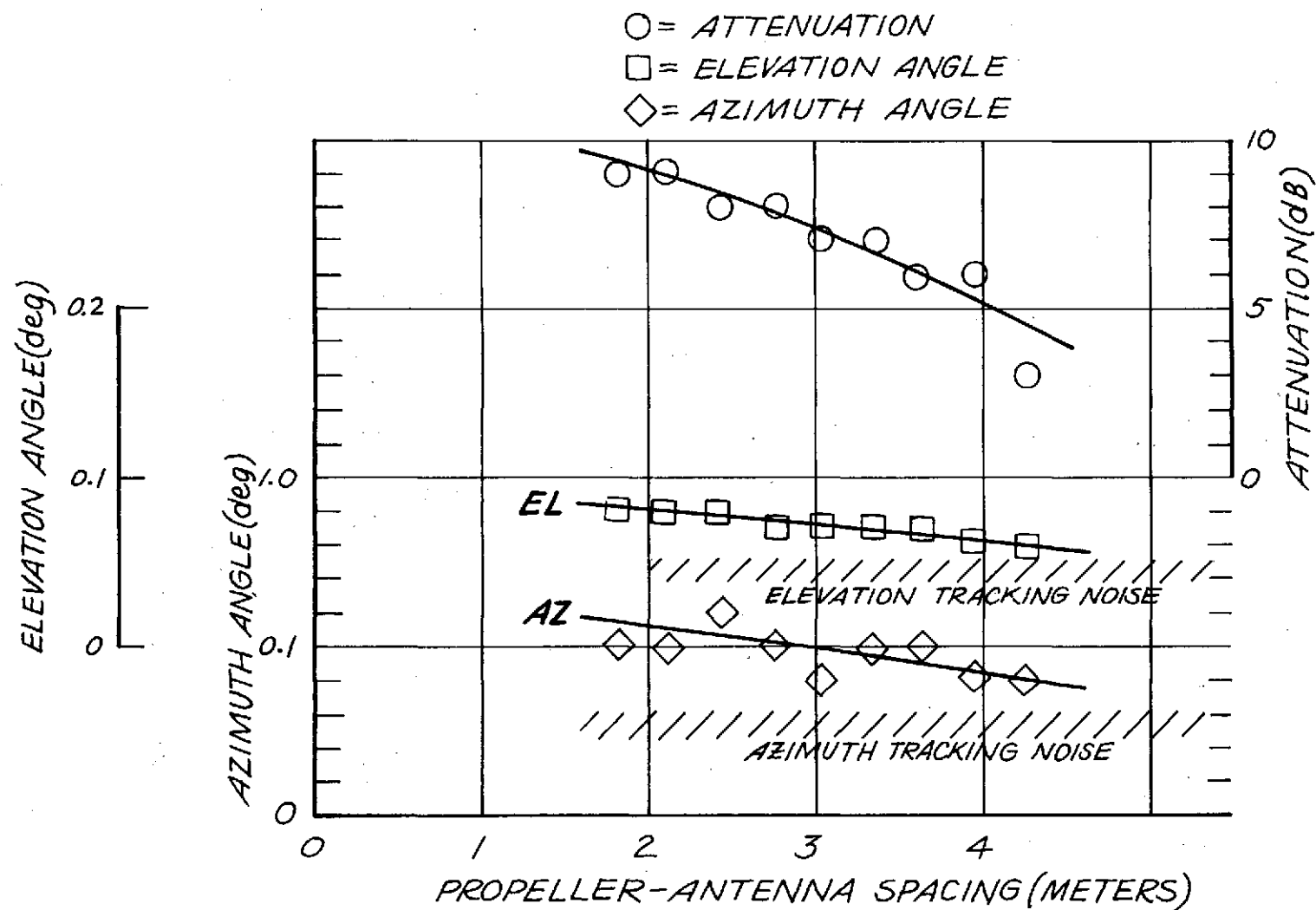
FIGURE 15. AGC AND ANGLE PEAK-TO-PEAK ERRORS VERSUS PROPELLER-RECEIVING ANTENNA SPACING.
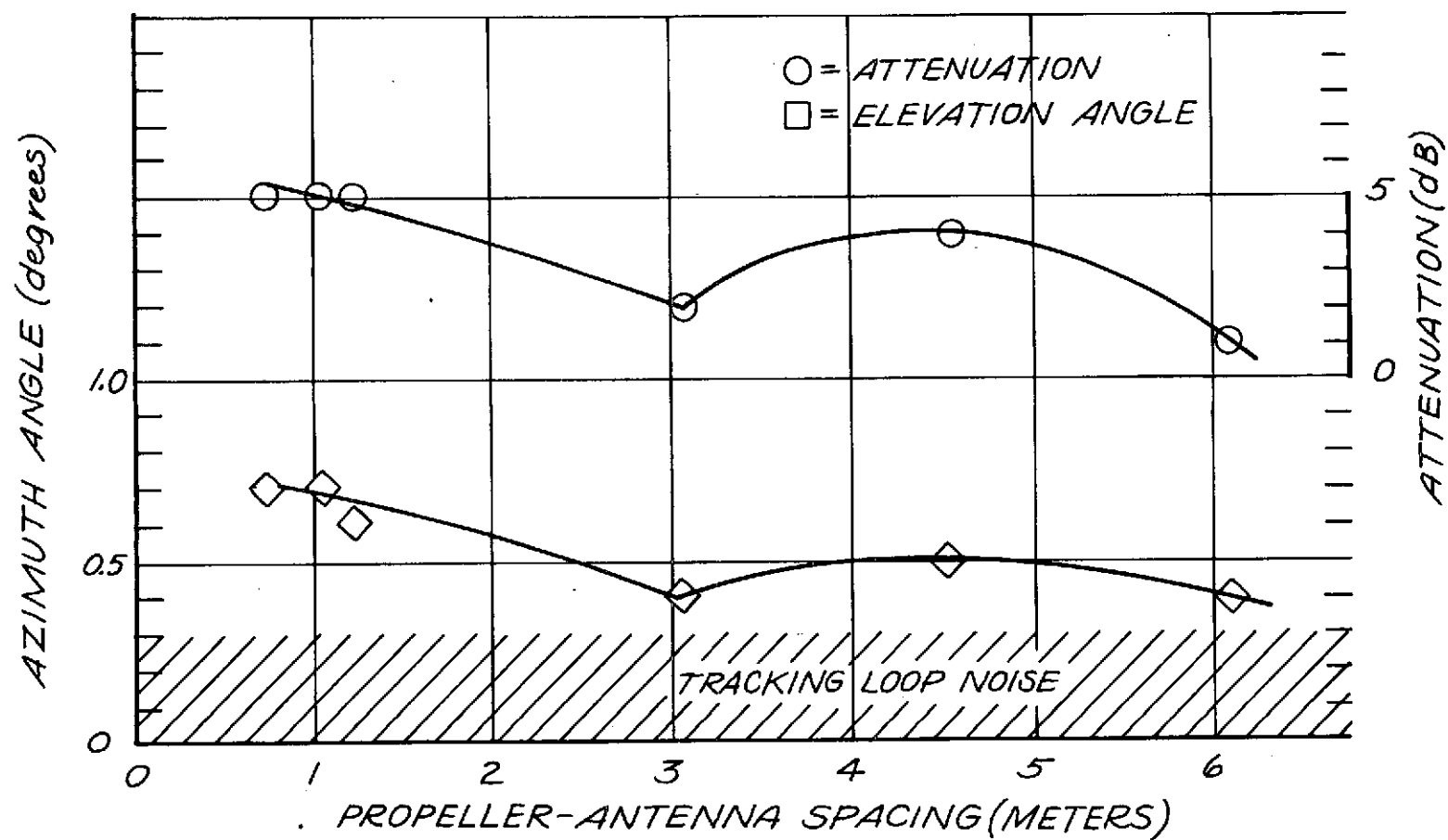
FIGURE 16. AGC AND AZIMUTH ANGLES PEAK-TO-PEAK
ERRORS VERSUS PROPELLER-RECEIVING
ANTENNA SPACING AT CROWS LANDING

AZIMUTH ANGLE

BLADE
WIDTH
10.16
cm

4dB
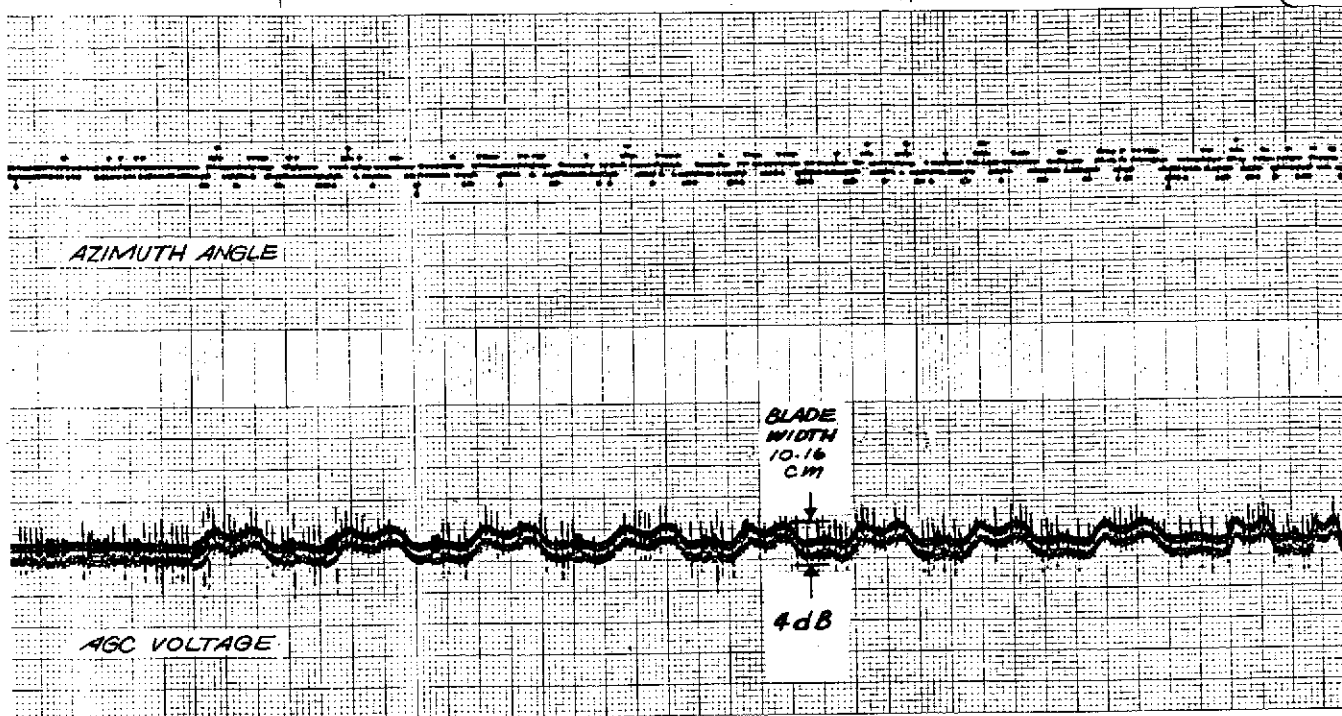
AGC VOLTAGE

FIGURES 17 - ANGLE AND AGC VOLTAGE ERRORS WITH TWO DIFFERENT
and 18.   BLADE WIDTHS AT A FIXED PROPELLER ANTENNA SPACING

AZIMUTH ANGLE

SPEED
CHANGE

BLADE
WIDTH
15.24
cm

5dB
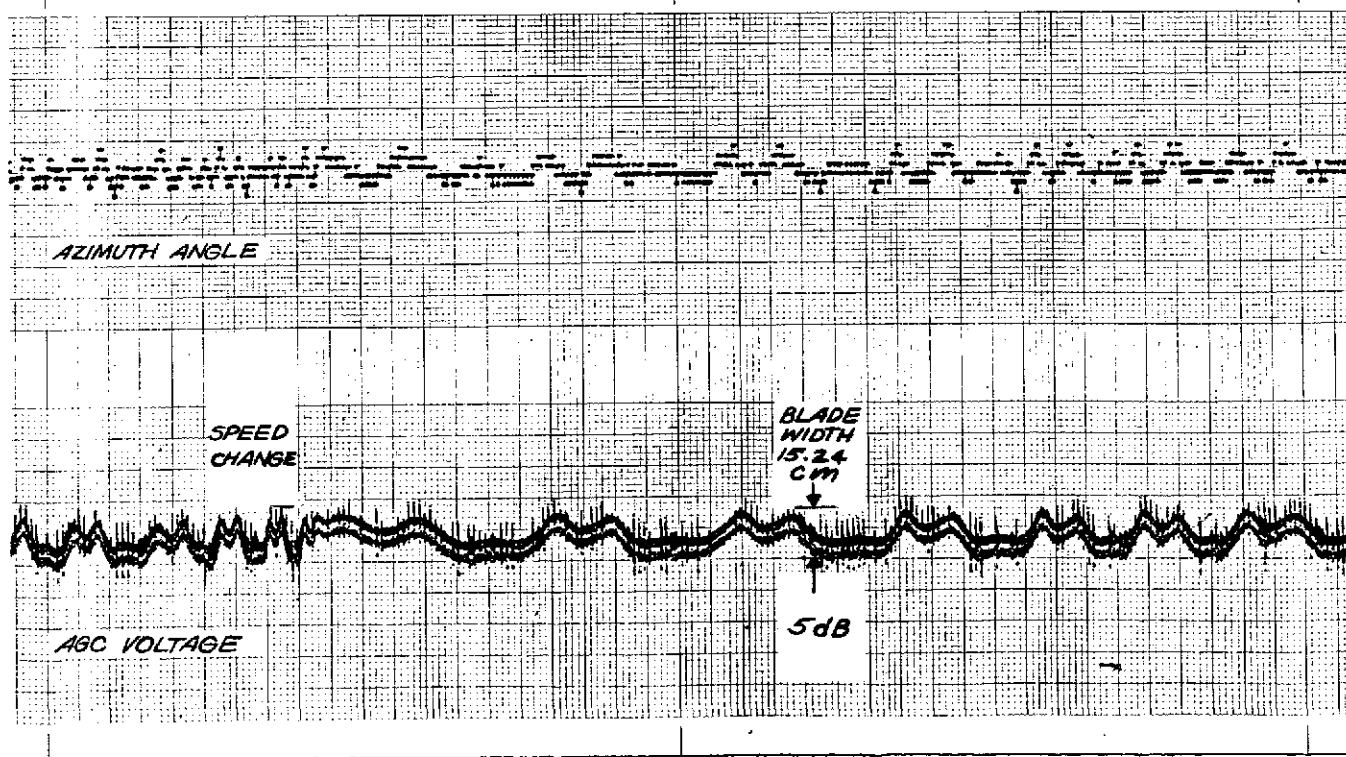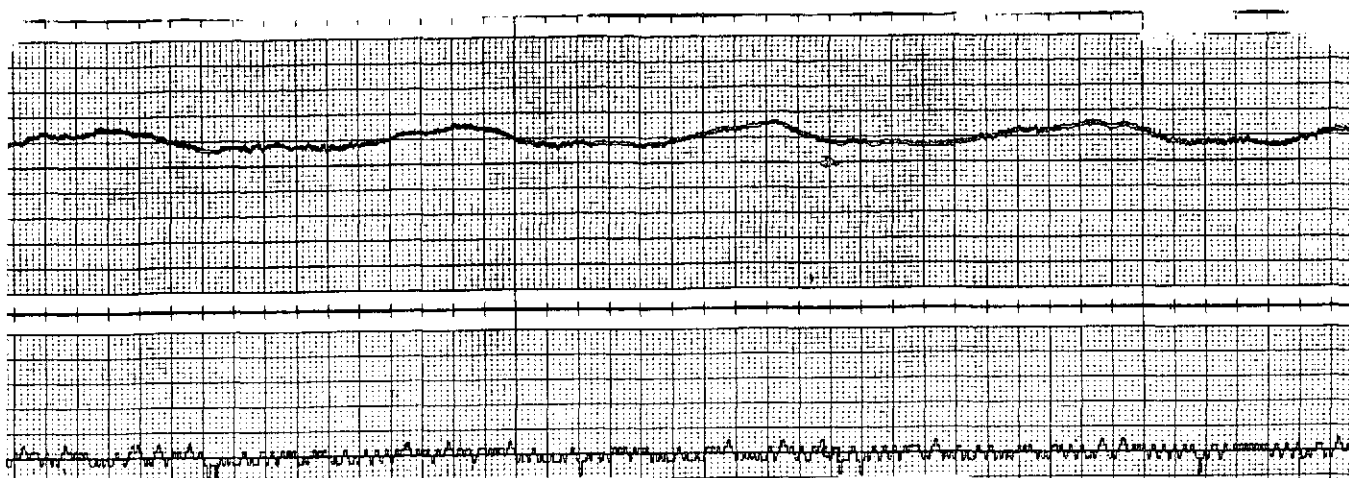
AGC VOLTAGE

FIG. 19 AGC VOLTAGE AND AZIMUTH ANGLE
ERRORS VERSUS BLADE INTERRUPT
DISTANCE(d) FROM PROPELLER TIP(d=0 cm)
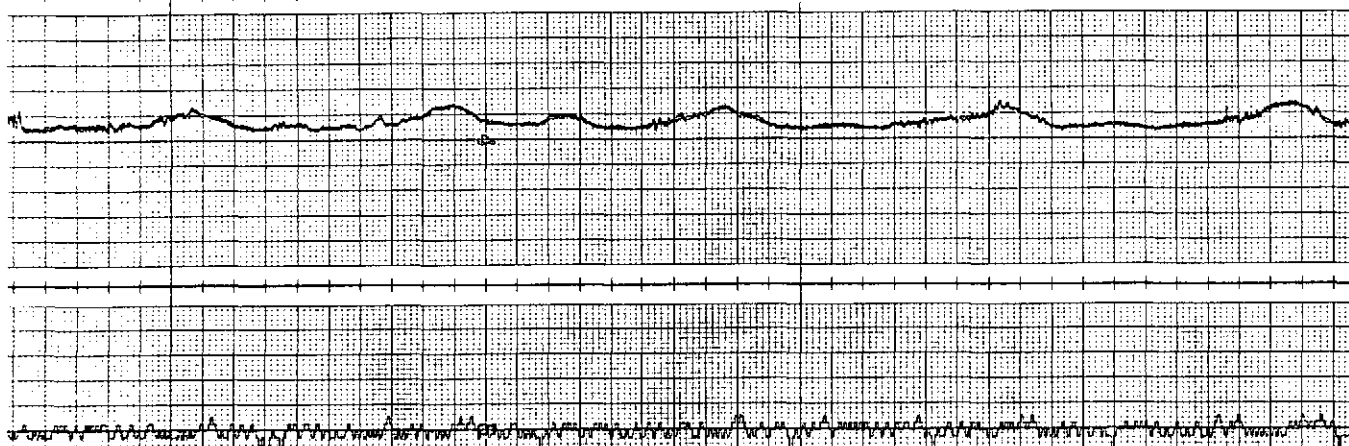
FIGURE 20 - AGC VOLTAGE AND AZIMUTH ANGLE
VERSUS BLADE INTERRUPT
DISTANCE (d = 2.5 cm)
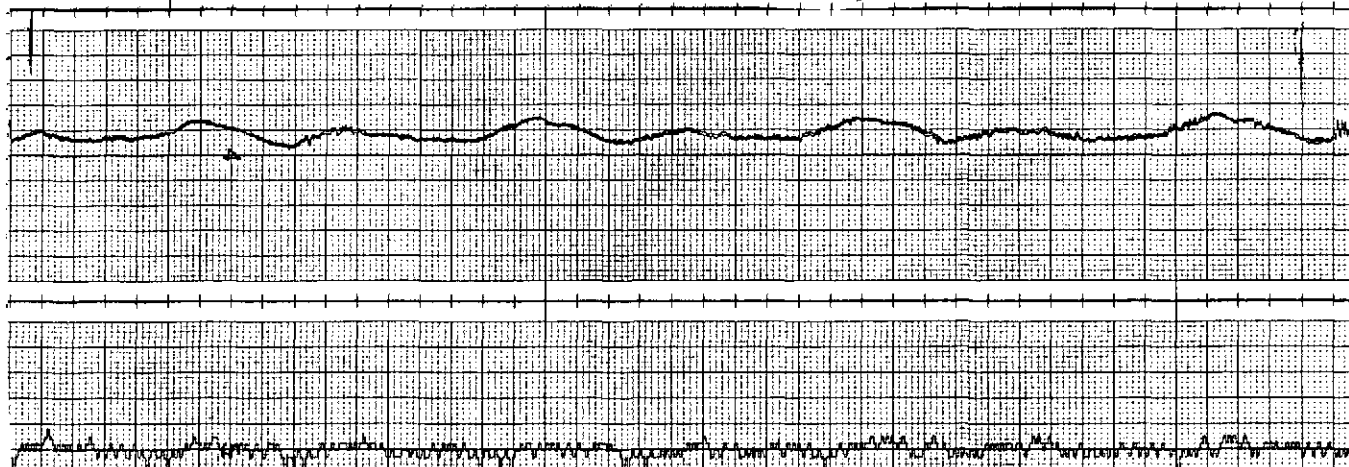
FIGURE 21 - AGC VOLTAGE AND AZIMUTH
ERRORS VERSUS BLADE
INTERRUPT DISTANCE(d = 8.9 cm)
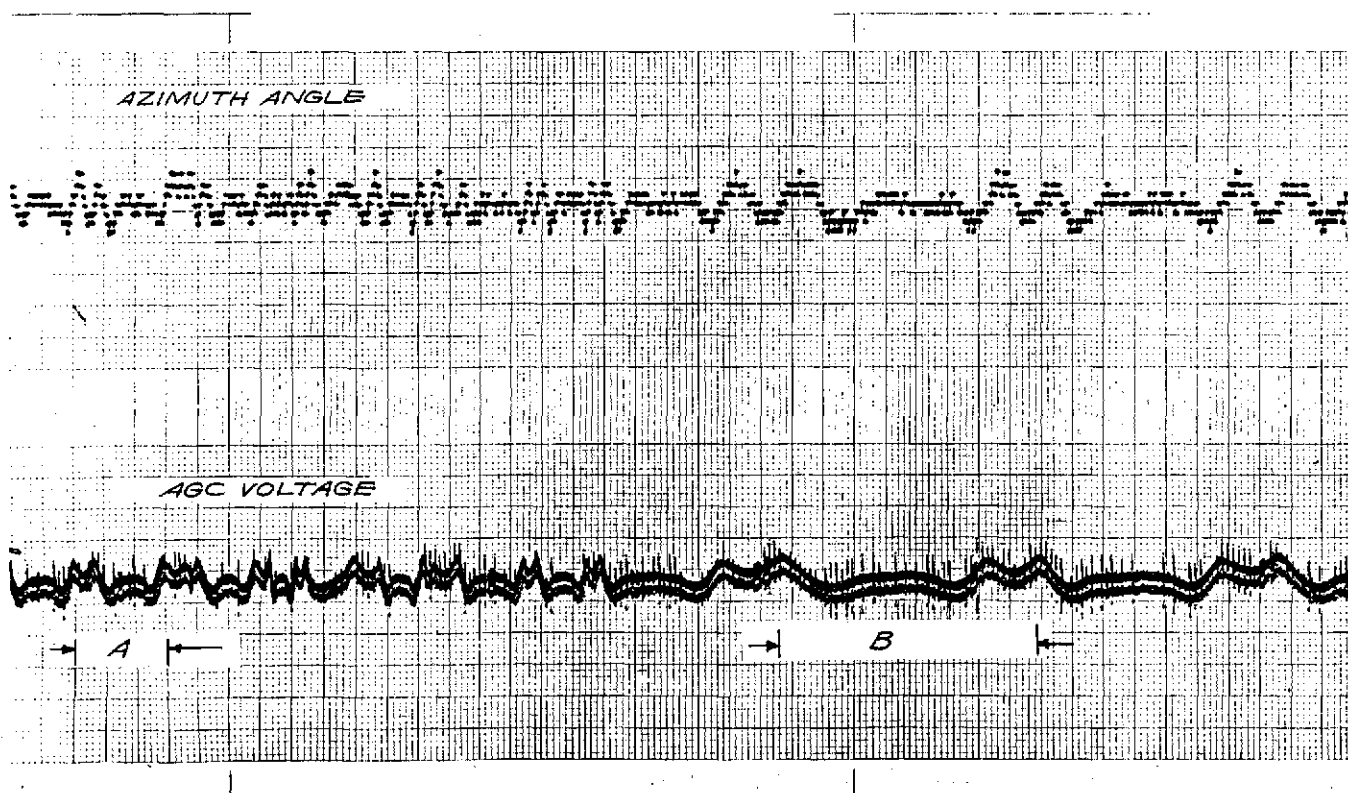
FIGURE 22. VARIATION OF PROPELLER MODULATION
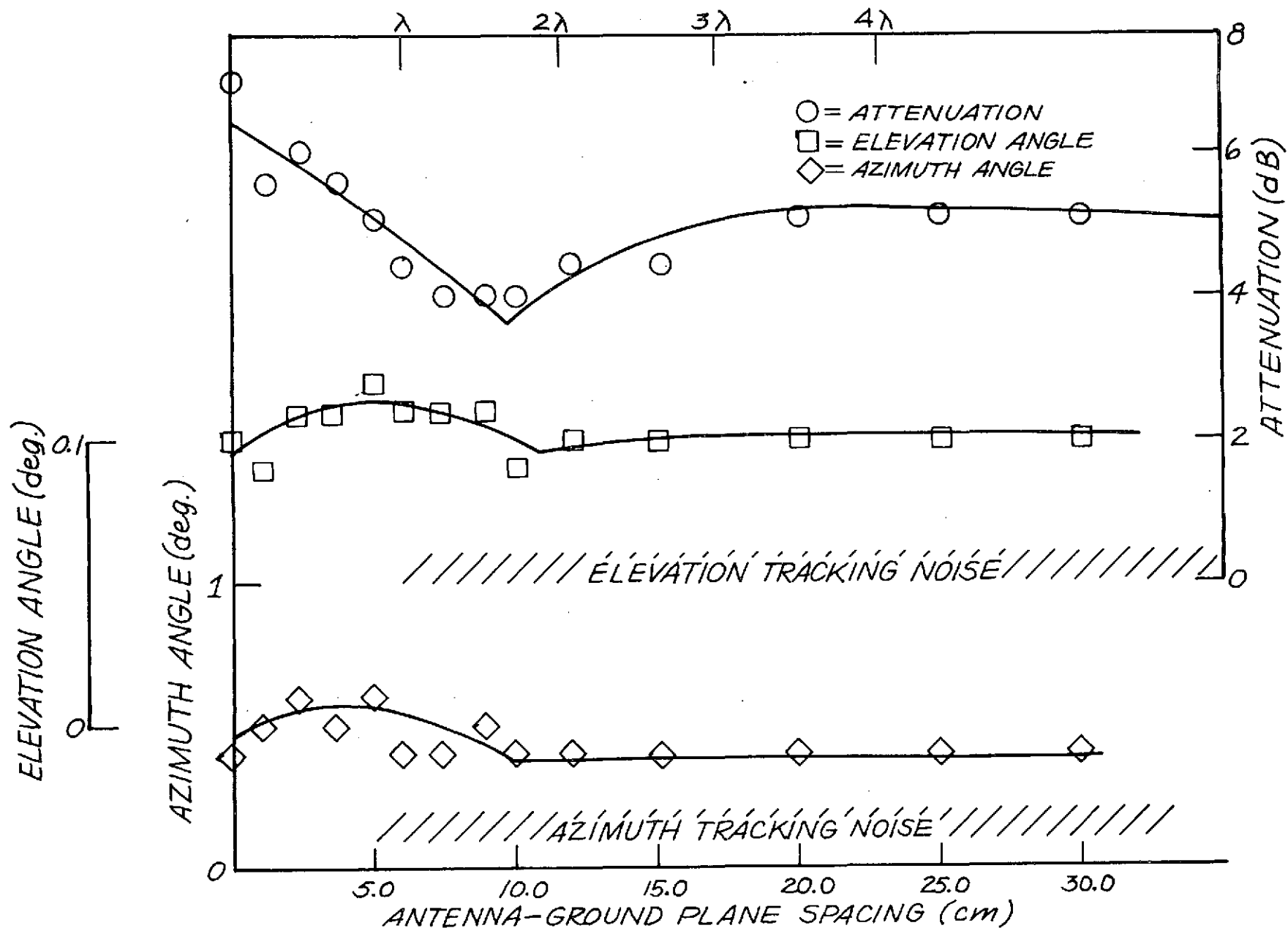   INTERFERENCE PERIOD WITH PROPELLER
         SPEED.

FIGURE 23.- PEAK-TO-PEAK ANGLE AND RECEIVED SIGNAL STRENGTH VARIATIONS VERSUS GROUND PLANE SPACING.
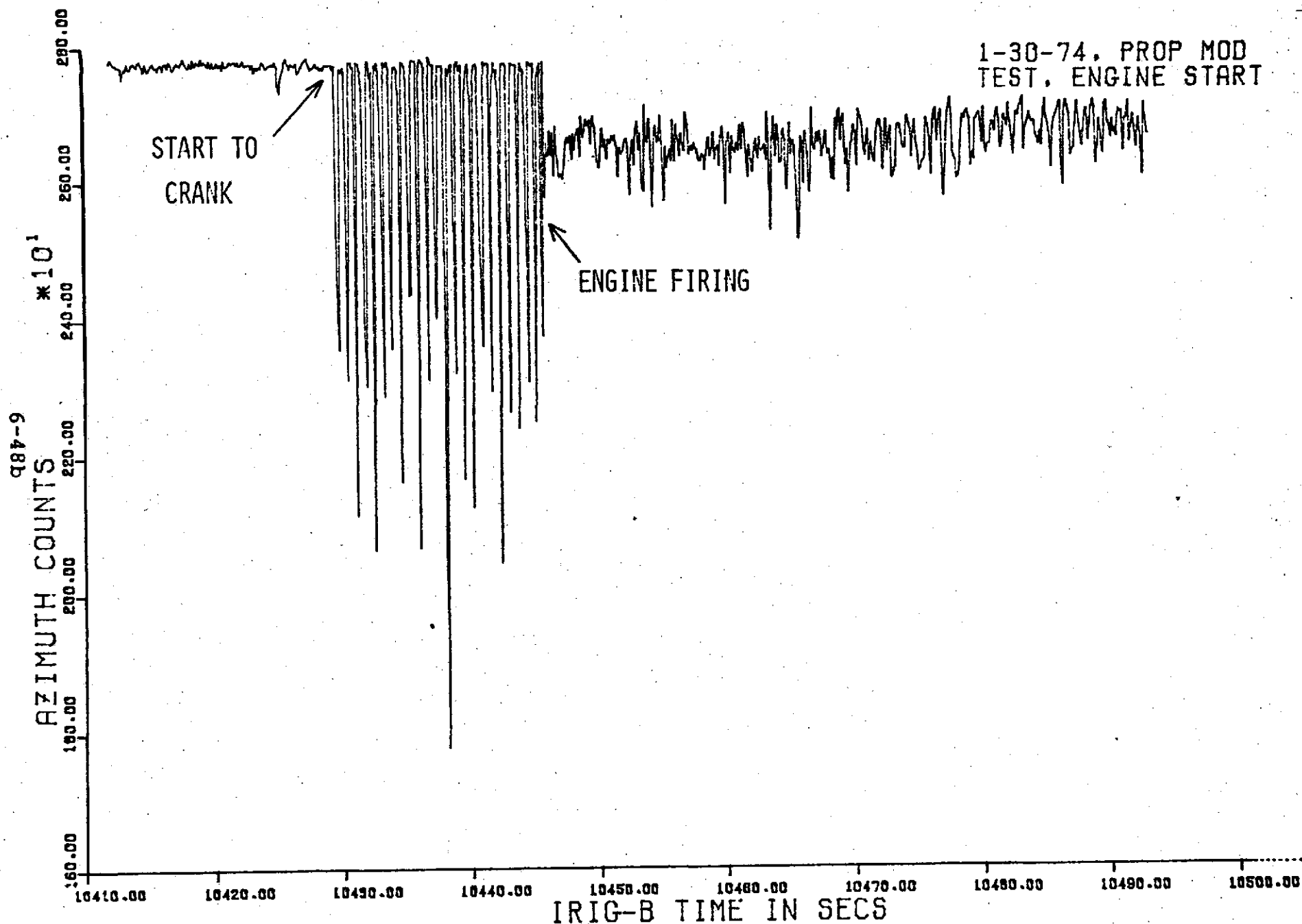
FIGURE 24. DOPPLER MLS AZIMUTH ANGLE VARIATIONS
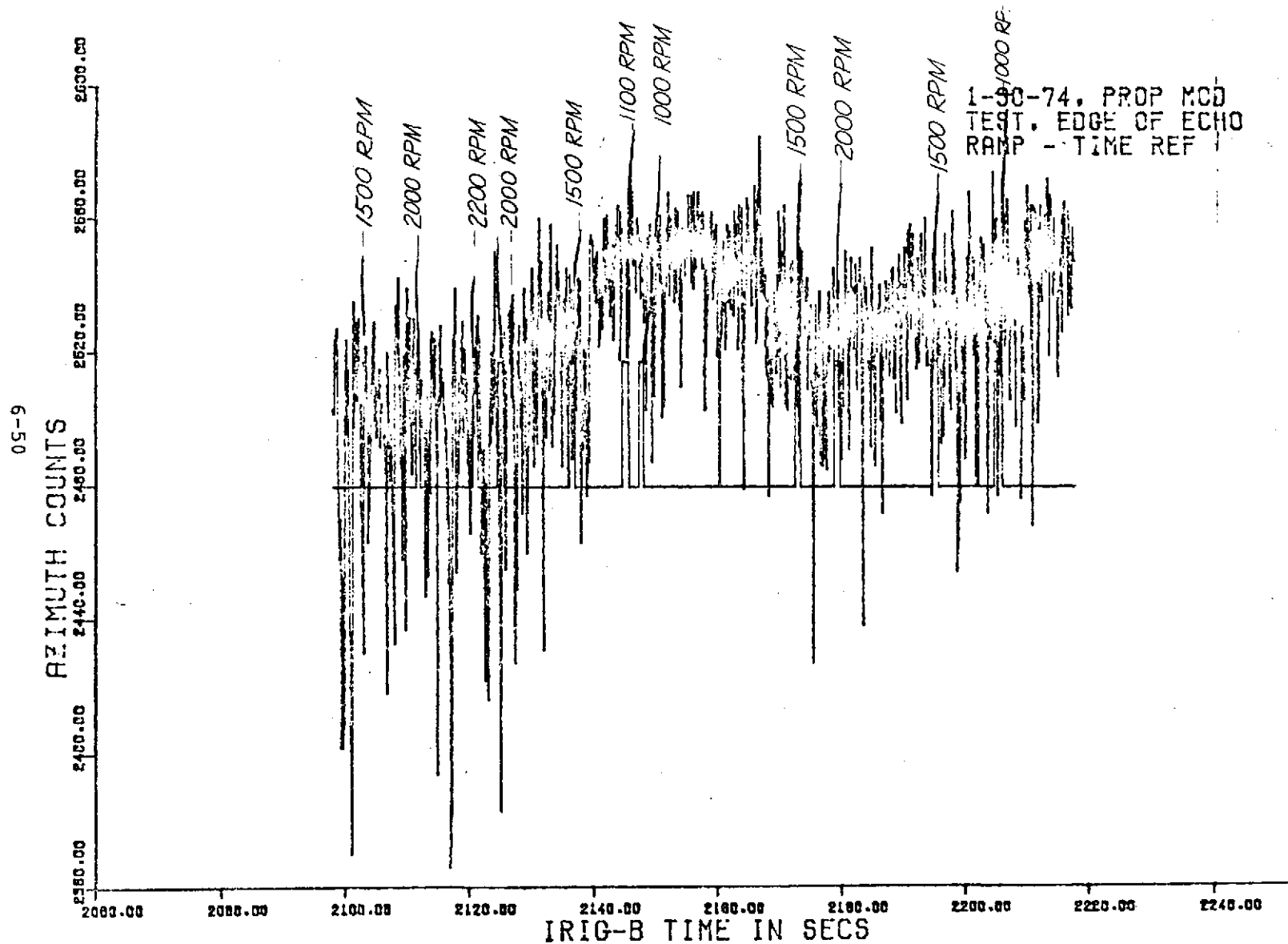AFTER ENGINE START USING A C131 AIRCRAFT.

FIGURE 25. DOPPLER MLS AZIMUTH ANGLE VARIATIONS
WITH CHANGES IN ENGINE RPM